diversity

MDPI

Article

Microbial Communities of Ferromanganese Sedimentary Layers and Nodules of Lake Baikal (Bolshoy Ushkany Island)

Tamara Zemskaya [1], Natalia Konstantinova [2,3], Olga Shubenkova [1], Tatyana Pogodaeva [1], Vyacheslav Ivanov [1], Sergei Bukin [1], Andrey Khabuev [1], Oleg Khlystov [1], Grigory Vilkin [2] and Anna Lomakina [1,*]

[1] Limnological Institute, Siberian Branch of the Russian Academy of Sciences (LIN SB RAS), 664033 Irkutsk, Russia
[2] Institute for Geology and Mineral Resources of the Ocean (VNIIOkeangeologia), 190121 St. Petersburg, Russia
[3] Far East Geological Institute FEB RAS, 690022 Vladivostok, Russia
* Correspondence: lomakina@lin.irk.ru

Abstract: Ferromanganese (Fe-Mn) sedimentary layers and nodules occur at different depths within sediments at deep basins and ridges of Lake Baikal. We studied Fe-Mn nodules and host sediments recovered at the slope of Bolshoy Ushkany Island. Layer-by-layer ^{230}Th/U dating analysis determined the initial age of the Fe-Mn nodule formation scattered in the sediments as 96 ± 5–131 ± 8 Ka. The distribution profiles of the main ions in the pore waters of the studied sediment are similar to those observed in the deep-sea areas of Lake Baikal, while the chemical composition of Fe-Mn nodules indicates their diagenetic formation with hydrothermal influence. Among the bacteria in microbial communities of sediments, members of organoheterotrophic *Gammaproteobacteria*, *Chloroflexi*, *Actinobacteriota*, *Acidobacteriota*, among them *Archaea*—chemolithoautotrophic ammonia-oxidizing archaea *Nitrososphaeria*, dominated. About 13% of the bacterial 16S rRNA gene sequences in Fe-Mn layers belonged to *Methylomirabilota* representatives which use nitrite ions as electron acceptors for the anaerobic oxidation of methane (AOM). *Nitrospirota* comprised up to 9% of the layers of Bolshoy Ushkany Island. In bacterial communities of Fe-Mn nodule, a large percentage of sequences were attributed to *Alphaproteobacteria, Actinobacteriota* and *Firmicutes*, as well as a variety of OTUs with a small number of sequences characteristic of hydrothermal ecosystems. The contribution of representatives of *Methylomirabilota* and *Nitrospirota* in communities of Fe-Mn nodule was minor. Our data support the hypothesis that chemolithoautotrophs associated with ammonium-oxidizing archaea and nitrite-oxidizing bacteria can potentially play an important role as primary producers of Fe-Mn substrates in freshwater Lake Baikal.

Keywords: microbial communities; diversity of 16S rRNA sequences; Fe-Mn nodules; deep sediments; Lake Baikal; chemical composition

Citation: Zemskaya, T.; Konstantinova, N.; Shubenkova, O.; Pogodaeva, T.; Ivanov, V.; Bukin, S.; Khabuev, A.; Khlystov, O.; Vilkin, G.; Lomakina, A. Microbial Communities of Ferromanganese Sedimentary Layers and Nodules of Lake Baikal (Bolshoy Ushkany Island). *Diversity* **2022**, *14*, 868. https://doi.org/10.3390/d14100868

Academic Editor: Roberto Pizzolotto

Received: 6 September 2022
Accepted: 11 October 2022
Published: 13 October 2022

1. Introduction

Fe-Mn deposits such as crusts, nodules and micronodules are composed of iron and manganese oxides and hydroxides and are widespread in both continents and the global ocean, including abyssal plains, deep-sea seamounts and ridges, shallow-water seas and freshwater lakes [1–8]. Both abiotic and microbiological processes play an important role in the precipitation of iron and manganese oxyhydroxides (e.g., [9–16]). Marine Fe-Mn deposits are formed as precipitates sourced from cold seawater (hydrogenetic), sediment porewaters (diagenetic) and fluids of submarine volcanoes at spreading centers and other tectonically active areas (hydrothermal) (e.g., [17–19]). There are significant variations in the chemical and mineral composition between types of Fe-Mn deposits. Crusts and nodules strongly affect the metal and organic accumulation in the ocean due to their high reactivity and oxidizing abilities [20–23]. Hydrogenetic mineralization occurs on hard-rock substrates of seabed seamounts, ridges and plateaus, and is enriched in rare earth elements (REE) and trace elements. Diagenetic influence is reflected in higher contents of

Cu, Ni, Zn, Li, Mo, and Cd, and hydrothermal deposits usually show low concentrations of minor metals [24]. Shallow-water Fe-Mn deposits do not accumulate rare elements, are enriched in iron in relation to manganese and are characterized by a high content of detritus (e.g., [25,26]). Lake nodules reflect the local environment, including the composition of water and sediments. For instance, some Fe-Mn nodules from lakes accumulate As, Ba, Ce, Eu, La, Sm, Sr, Th, and U [27,28], but, in general, lake deposits are depleted in trace elements and have an increased Fe/Mn ratio [3].

The biogenesis process in the formation of Fe-Mn deposits has not been fully described and the data on microbial communities and their interrelation in crusts are limited, although the biological contribution to the formation of Fe-Mn deposits is beyond any doubt [9,12,13]. Microorganisms may be potentially involved in the transition of elements between seawater and Fe-Mn substrates [13,16,29], as well as in the oxidation and precipitation of Mn. The microbial diversity and abundance were studied in Fe-Mn crusts, host sediments throughout the global ocean [9,12,13,21,30,31]. Bacteria and archaea associated with the oxidation of nitrogen compounds, such as *Nitrospirota*, *Nitrospinota* phyla and *Candidatus* Nitrosopumilus in the class *Nitrososphaeria* occur, as well as numerous associations involved in methane oxidation, i.e., *Methylomirabilales* (formerly NC10) and SAR324 (*Deltaproteobacteria*). Chemolithoautotrophs associated with ammonia-oxidizing archaea and nitrite-oxidizing bacteria may potentially play an important role as primary producers of Fe-Mn crusts at Rio Grande Rise (RGR) [9]. The analysis of 16S rRNA gene libraries of Fe-Mn deposits from different regions of the World Ocean indicate a variety in composition of microbial communities compared to seawater [32] and the presence of phylogenetically different sequences of one taxon [9]. Metagenomic sequencing of Fe-Mn crust confirmed the presence of the putative genes in the metagenome, which are involved in the dissolution and precipitation of Fe and Mn, nitrification, sulfur oxidation, carbon fixation, and decomposition of organic matter [13].

Microbial communities associated with freshwater Fe-Mn deposits are not well studied [29,33–37]. Chemical composition and morphology of Fe-Mn micronodules indicate diagenetic transformations involving the activity of microorganisms [21,22,33]. Bacterial cultivation experiments confirmed the capacity to precipitate oxidized Fe and Mn [38–40]. Mn oxides of the crust in freshwater neutral pH environment are considered to be biogenic, but the microbial community composition and its influence on crust formation there remain unclear [41]. High-throughput sequencing of bacteria and eukaryotes, including fungi, revealed that black Mn crusts in the oligotrophic environment of the Kurokawa River contain a great number of the genera *Sphingomonas*, *Hyphomicrobium*, *Bacillus*, *Pseudomonas*, and *Mortierella*, including several Mn-oxidizing species in the Mn crusts or nodules of sea and fresh waters. Microbial communities in Fe-enriched sediments of Lake Superior showed the dominance of the phylum *Methylomirabilota*, which are anaerobic methane oxidizers, and the *Nitrospira* species that are the most similar to bacteria from Fe-enriched seeps [42]. The iron-enriched sediment layers of Lake Constance formed during nitrate-dependent anaerobic oxidation [43]. Wang & Muller [16] suggested that free-living and biofilm-forming bacteria serve as a matrix for Mn precipitation, and coccolithophores are the dominant organisms that act as a matrix (bioearth) for the initial Mn precipitation in Fe-Mn crusts. On the contrary, some authors believe these endolithic and epilithic microbial communities use Fe-Mn crust as a favorable physical substrate [32,44,45].

Iron and manganese mineralization in Lake Baikal occurs in the form of sediment layers or nodules and is widespread in all three basins, as well as on the Academic Ridge [33]. The dynamics of Fe-Mn layers were presumably caused by past climatic changes [46] or by tectonic events and subsequent redistribution of Fe and Mn [37]. Och et al. [29] suggested a mechanism of diagenetic Fe-Mn mineralization: dynamic formation of Fe and Mn layers at the lower end of the oxygen penetration depth, and slowly reductive dissolution of Mn(IV) occurred at the lower margin. Upward-diffusing Mn(II) was oxidized with O_2 forming the new dynamic Fe-Mn layers above. The dissolution of the buried Fe-Mn oxide layer is ultimately controlled by AOM with SO_4^{2-} and/or Fe oxides in deeper sediments

and by the formation of the upper dynamic Fe-Mn oxide layer due to the diffusion flux of O_2 from the water column into the sediments [29]. The biogenic influence on Fe-Mn layers throughout their diagenetic formation in freshwater sediments of Lake Baikal is supported by studies by Dubinina [47], Granina [33] and Zakharova et al. [48]. The occurrence of cultivated Fe- and Mn-oxidizing bacteria in the bottom sediments of Lake Baikal was shown, as well as the relationship between bacteria distribution and abundance and redox conditions, organic matter contents, and dissolved Fe and Mn in pore waters. Members of the six genera *Metallogenium*, *Leptothrix*, *Siderocapsa*, *Naumaniella*, *Bacillus*, and *Pseudomonas* were involved in the oxidation of Fe(II) and Mn(II) in the bottom sediments of Lake Baikal [48]. High-throughput sequencing of microbial communities of the sediments with Fe-Mn layers from southern Baikal basin allowed the relation between changes in their structure and geochemical conditions to be defined, while the most significant differences in the structure of the microbial communities are in Fe-Mn layer [49]. These studies did not observe typical for communities of freshwater ecosystems members of AOM (ANME-2d and NC10), reflecting the dominance of ammonium oxidizing archaea (*Nitrososphaeria*), although the former are widespread in sediments from other areas of Lake Baikal.

Despite the fact that hydrothermal vent activity has not yet been discovered at the Bolshoy Ushkany Island site, its influence on Fe-Mn nodules from the slope of Bolshoy Ushkany Island was suggested previously [33,50,51]. Nodules collected by a PISES manned submersible at the intersection of neotectonic faults, where bottom waters have enhanced electrical conductivity, had high Mn concentrations and were also significantly enriched in Ni, Cu, and Ba [33,50,52,53]. In addition, the hydrothermal precipitate geyserite was observed at this site and at the Frolikha vent [54]. During the 2019 expedition on the northern slope of Bolshoy Ushkany Island, we collected Fe-Mn nodules and bottom sediments which are the subject of our research.

Here we (i) report on the chemical composition, genesis and age of Fe-Mn nodules, the chemical composition of pore water, as well as the structure and diversity of microbial communities in the sediments and nodules using high-throughput sequencing and (ii) discuss the contribution of microorganisms involved in the anaerobic oxidation of methane, nitrogen and sulfur cycles as possible participants of dissolution/precipitation of the buried Fe-Mn oxide layer according to the hypothesis of Och et al. [29].

2. Materials and Methods

2.1. Sample Collection

Sediments and nodules were collected by NIOZ-type box core (Grf), rectangular in shape, 0.78 m^{-2}, and 70 cm high from the site located on the northern slope of Bolshoy Ushkany Island (53.884673 N, 108.615265 E, St6 Grf7) at 650 m water depth (Figure 1). The expedition was carried out using R/V "G. Yu. Vereshchagin" in 2019. T chemical analysis of pore waters, methane concentration and lithology were carried out in the laboratory on board the vessel. The sediments sampled for DNA extraction were stored in liquid nitrogen until the laboratory analysis. Age dating of Fe-Mn nodules was carried out also in the laboratory. For the chemical analysis and molecular investigation, the surface layer 0–1 cm, 9–10 cm (Fe-Mn layer), 10–11 cm, 11–12 cm, 22–23 cm, and four Fe-Mn nodules (Samples 1–4) were taken. Nodules were located at the different depths within sediments and on the sediment surface.

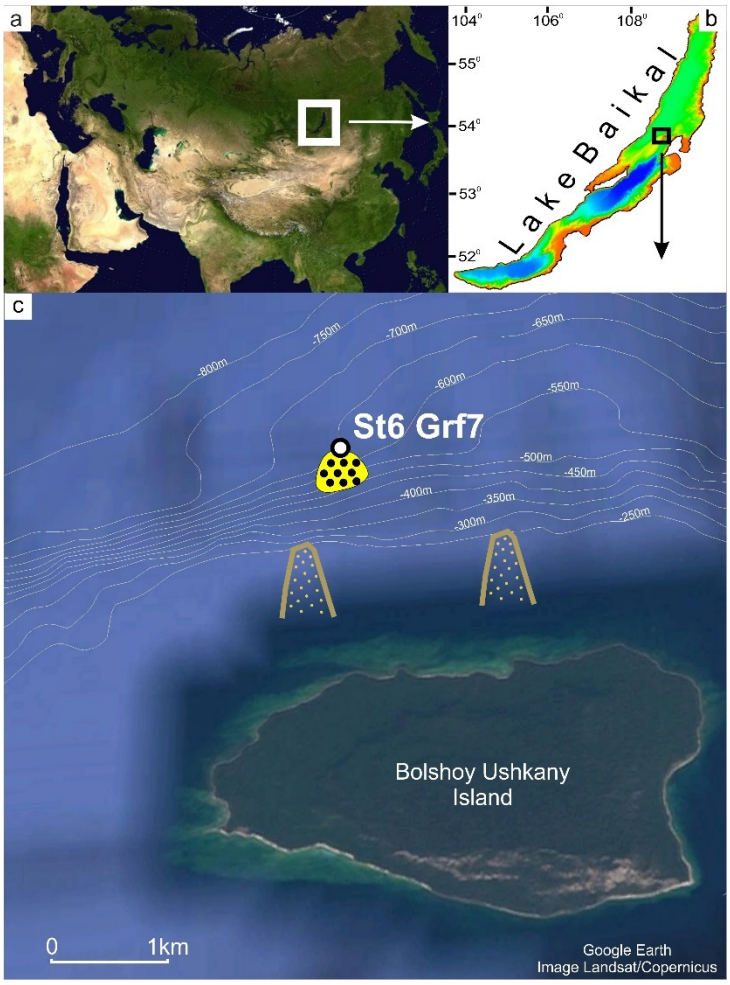

Figure 1. (**a**) Geographic location of Lake Baikal; (**b**) Geographic location of Bolshoy Ushkany Island; (**c**) Area of sampling sediments and Fe-Mn deposits (St6 Grf7). Light brown shows the slope slides.

2.2. Chemical Analysis

Pore water extractions were obtained from samples (100 g each) on board the ship by sequentially centrifuging the sample for 20 min at 5000× *g* and then for 10 min at 12,000× *g*. Chemical analysis was carried out as described previously [55]. The pore water anion and cation contents were determined at the Collective Instrumental Center "Ultramicroanalysis" of LIN SB RAS. Pore water anion (SO_4^{2-}, NO_3^-, HCO_3^-, and CH_3COO^-) concentrations were measured onboard the ship by liquid chromatography using Milikhrom-A-02 (Novosibirsk, Russia) immediately after preparation (relative error 5–10%) [56]. Cation (Na^+, K^+, Ca^{2+}, and Mg^{2+}, Mn^{2+}, Fe^{2+}) concentrations were determined using atomic absorption and flame emissivity methods (relative error 3–5%). NH_4^+ was determined onboard by colorimetric methods (relative error 5%). Measurements of pH and Eh were carried out in sediments using pH 3310 ("WTW", Oberbayern, Germany).

The chemical composition of four Fe-Mn nodules (Si, Al, Ca, Fe, K, Mg, Mn, Na, P, Ti, Li, Be, Sc, V, Cr, Co, Ni, Cu, Zn, Ga, Ge, As, Se, Rb, Sr, Y, Zr, Nb, Mo, Ag, Cd, Sb, Cs, Ba, REE, Hf, Ta, W, Tl, Pb, Th, and U) were determined by inductively coupled plasma mass-spectrometry (ICP-MS) using Agilent 7700x (Agilent Technologies) and by inductively coupled plasma atomic emission spectroscopy with iCAP6500 Duo (ThermoScientific) in the laboratory of Far East Geological Institute in Vladivostok. Rare Earth Element and Yttrium (REY) distribution plots were used for studying Fe-Mn deposit genesis and were normalized to shale (PAAS, Post-Archean Australian Shale) [57]. The Ce anomaly was calculated as Ce* = 2Ce/(La + Pr) for PAAS-normalized values.

The distribution of chemical elements in the mineral phases of Fe-Mn nodules was studied for two samples (Samples 1 and 2) using the method of sequential leaching, which uses the procedure described in Konstantinova et al. [58], Koschinsky and Halbach [59], Koschinsky and Hein [60], and Mikhailik et al. [61]. Four mineral phases of different stability were dissolved step-by-step: exchangeable cations and Ca carbonates, Mn-oxides, Fe-hydroxides, and residual aluminosilicate fraction. The solutions obtained were analyzed by ICP AES and ICP MS in the Center for Collective Use of the Far Eastern Geological Institute.

2.3. Age Dating

The ^{230}Th/U dating method was used to determine the age and average growth rate of the two samples (Samples 1 and 3). The ^{238}U, ^{234}U, ^{232}Th, and ^{230}Th isotopes were measured using alpha-spectrometer "Alpha Duo" (ORTEC). The detailed chemical procedure and counting techniques are described in Kuznetsov et al. [62]. The measurements were carried out in sublayers with a step of 2 mm in laboratory "Palaeogeography and geomorphology of Polar Countries and the World Ocean" of St. Petersburg State University.

2.4. Methane Concentration

Methane concentration in the gaseous phase was determined by the Headspace method [63] on an EKHO-PID chromatograph (Russia) (flame ionization detector, 2 m packed column with an inner diameter of 2 mm; Porapak Q sorbent, isothermal mode, column temperature 100 °C, injector temperature 100 °C, and detector 150 °C). The gas volume was 0.5 mL. The error of the determination method is 7%.

2.5. Molecular Microbiological Methods

Sediments for DNA extraction were sampled immediately after collection: 10 g of sediments were packed in sterile foil and placed in liquid nitrogen until laboratory analysis.

DNA was extracted from sediments by enzymatic lysis, followed by phenol-chloroform extraction [64]. For the PCR amplification of 16S rRNA gene fragments of bacteria, including the variable region V2–V3, the universal primers, 16S_BV2f (5′-AGTGGCGGACGGGTGAG TAA-3′) and 16S_BV3r (5′-CCGCGGCTGCTGGCAC-3′) [65], as well as the following procedure, were used: 95 °C for 15 min; 96 °C for 30 s; 53 °C for 60 s; 72 °C for 40 s (25 cycles), and 72 °C for 10 m. For the PCR amplification of 16S rRNA gene fragments of archaea, the primers that included the variable region V5–V6, Arch-0787f (5′-ATTAGATACCCSBGTAGTCC-3′) and Arch-1059r (5′-GCCATGCACCWCCTCT-3′) [66], as well as the following procedure, were used: 95 °C for 15 m; 96 °C for 30 s, 50 °C for 60 s, 72 °C for 40 s (25 cycles), and 72 °C for 10 m. The libraries were analyzed using Illumina MiSeq Standard Kit v.3 (Illumina) at the Core Centrum "Genomic Technologies, Proteomics and Cell Biology" in ARRIAM.

The resulting paired-end sequencing reads were trimmed from the end to 270 bp using Trimmomatic version 0.39 [67] to remove positions, in which more than 25% of the reads had bases with relative quality scores < 20, calculated using FastQC v. 0.11.9 [68]. The R1 and R2 sequences were then merged into contigs, filtered by size and average quality score ($\geq$25), aligned, and checked for chimeras against SILVA 138 databases (http://www.arb-silva.de, accessed on 1 February 2022) using the Mothur v.1.34.4 software [69] and the UCHIME algorithm [70]. Thereafter, the gaps were removed, and the sequences were tested for the presence of respective forward/reverse primers, allowing for two mismatches between the forward and reverse primer and sequence. Further 16S rRNA sequence processing was performed according to MiSeq SOP recommendations [71]. The filtered sequences were aligned, clustered and identified taxonomically using the SILVA 138 databases. After clustering, operational taxonomic units (OTUs) at a cluster distance level of 0.03 containing < 5 sequences across all samples were discarded. All calculations were performed on HPC-cluster "Akademik V.M. Matrosov". The 16S rRNA sequences

were deposited in the NCBI Sequence Read Archive under Bioproject PRJNA875570 and IDs SRR21383913-SRR21383923.

2.6. Data Analysis

Before analysis, all data on the concentration of ions in pore waters, as well as OTU relative abundance, were normalized by unitization with a zero minimum [(x-min)/range].

Comparisons of environmental parameters, alpha and beta diversity of microbial communities using principal coordinate analysis (PCoA), boxplots, heat maps and non-metric multidimensional scaling (NMDS), as well as statistical tests, were performed in R [72] with the vegan, stats, cluster, clusterSim, pheatmap, ggplot2, and ggbiplot packages.

3. Results

3.1. Properties of Sediments

3.1.1. Lithology

The length of sediment section of grab St6 Grf7 is 27 cm and it has the typical lithology for the study area (Figure 2a). An oxidized layer was observed from the surface to a depth of 17 cm with pH of 8.1, and Eh = +210.7 mV. Sediments are composed of brown diatom from the surface to 11 cm, decreasing the water cut with depth. A dark brown Fe-Mn layer occurs at a depth of 9–10 cm, which are similar to the layers Och et al. [29] indicated in deep-water sediments of other areas of Lake Baikal. The lower layer 10–11 cm was the layer after Fe-Mn layer. The sediments became light brown and contained some dark-colored spots attributed to the presence of Fe and Mn hydroxides in intervals of 13–20 cm. At depths of 20 to 27 cm, the sediments are composed of grey clay with dark inclusions and lenses. Fe-Mn nodules are observed throughout the section with the maximum abundance in the lower sand layer.

3.1.2. Chemical Composition of Pore Water

The pore water of the studied sediments is calcium bicarbonate, with mineralization ranging from 82.5 to 114 mg/L. Sulfate, nitrate and nitrite ions are detected throughout the sediment depth at concentrations varying from 3.0 to 5.6 mg/L, 1.06–1.42 mg/L and 0.09–0.15 mg/L, respectively (Figure 2b). The Mn ions profile demonstrates two peaks at depths of 9–10 cm, the interval of the upper Fe-Mn layer accumulation and 22–23 cm, where the buried Mn oxide layer forms. The profile of Fe ions has maximum values at a depth of 11–12 cm, reflecting the Fe-Mn (oxy)hydroxide mineralization and coinciding with numerous studies (e.g., [29]). Ammonium ions (0.03 mg/L) were presented only in the layer 22–23 cm (Figure 2b). The distribution profiles of other ions correspond to those observed in the deep-sea regions of Lake Baikal [29]. Methane concentrations at all sediment depths are below the instrument sensitivity (0.005 mg/L). Multidimensional scaling with PCoA confirms the different chemical composition of pore water in different sedimentary layers (Figure 2d). The samples do not form shared clusters, but are scattered along different axes.

3.2. Properties of Fe-Mn Nodules

3.2.1. Morphology

The most common morphology for the nodules discovered was disk-like flattened (length up to 6 cm, thickness up to 2 cm) (Figure 2c). Some of the nodules found had spherical and nodular shapes. Two types of nodules were identified: black, dense, often with a two-layered structure (Type 1; Samples 1–3) and reddish, and more fragile (Type 2; Sample 4) (Figure 2c). The surfaces of both types are usually smooth.

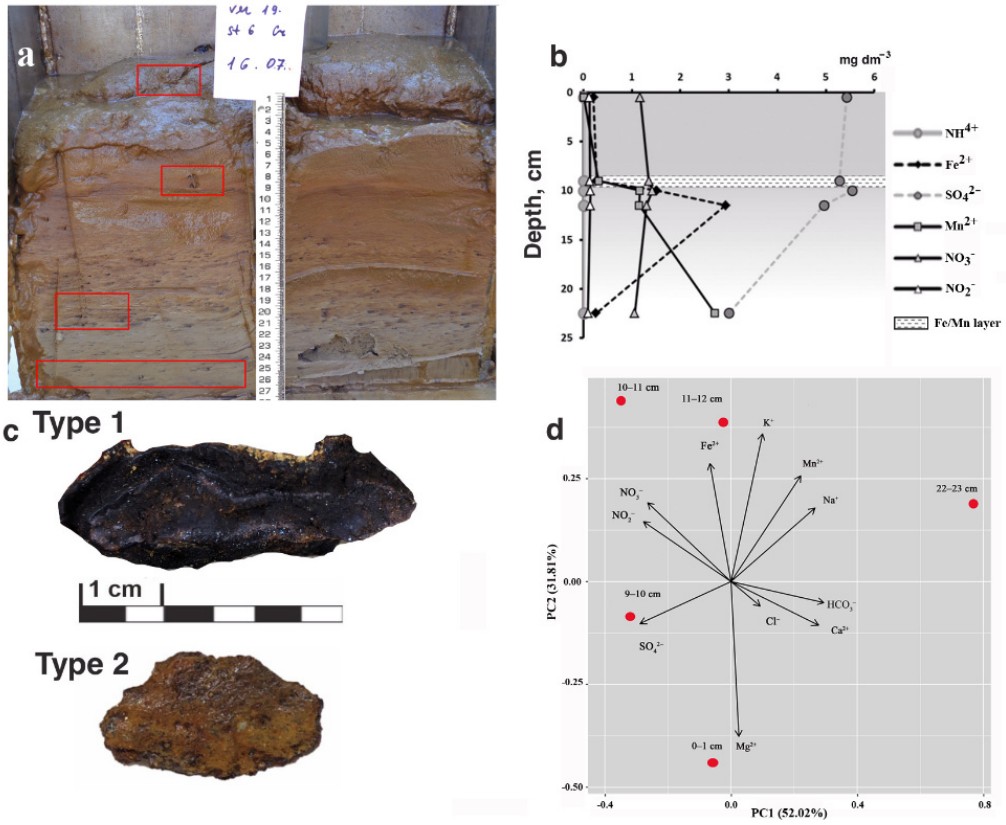

Figure 2. (**a**) Sediment section of grab St6 Grf7; red rectangles indicate Fe-Mn nodule locations throughout the sediment section; (**b**) Pore water concentration profiles; (**c**) Two morphological types of nodules: black, with a two-layered structure (Type 1) and reddish (Type 2); (**d**) Scatter plot of points in the space of two principal components based on the chemical composition of the pore water in different sedimentary layers. The arrows indicate the vectors directed along the gradients of changes in the parameters studied in the samples.

3.2.2. Chemical Composition

The content of the main elements (Fe, Mn, Co, Ni, Cu) in the nodules studied was lower than in the samples from the same area described earlier [53]. The mean Mn was 2.54%, Fe was 17.58%, Mn/Fe ratio was 0.14, Co was 56 ppm, Ni was 234 ppm, and Cu was 168 ppm. The Ni content exceeded Co by 4.2, which is typical for diagenetic nodules, in particular in the Clarion–Clipperton Zone [24]. The content of rare and rare-earth elements (REE) of nodules was insignificantly lower than the values observed in Fe-Mn nodules from different regions of the global ocean. Total REY for the bulk crusts varied from 280 ppm to 505 ppm. A key characteristic of the Baikal nodules was significantly higher U and Cr content than those in oceanic nodules [5,73] and samples from the southern Lake Baikal (Figure 3). Thus, the mean content of U was 36.2 ppm and Cr was 88.5 ppm in comparison with the mean data for crusts and nodules from other areas in the global ocean of U 10–13 ppm, Cr 16–46 ppm [5,73]. The high concentrations of uranium were also observed in the sediments of lake Baikal, U > 20 ppm [74,75] and U ~ 15 ppm [76].

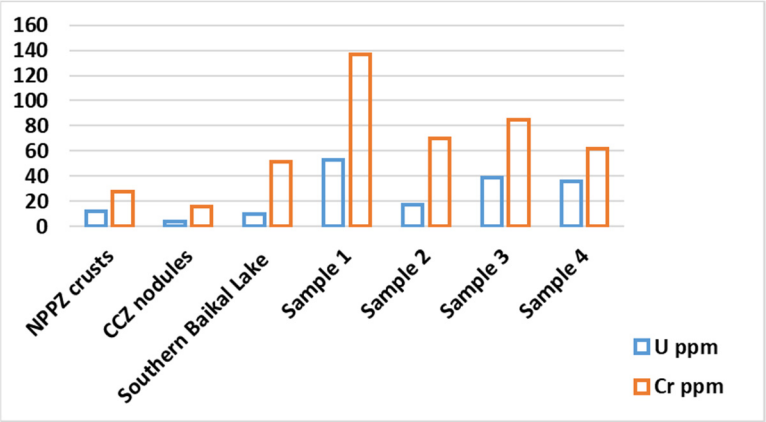

Figure 3. U and Cr concentrations in Fe-Mn nodules from the slope of Bolshoy Ushkany Island and the Southern basin of Lake Baikal (our data), cobalt-rich crusts from North Pacific Prime Zone (NPPZ) and nodules of the Clarion–Clipperton Zone in the Pacific Ocean (CCZ) [5,73].

The sequential leaching experiments showed that uranium is predominantly associated with iron mineral phase, represented by iron (oxy)hydroxides. The U percentage in the iron phase was constant and was about 60%, and was not reliant on the total U content in the sample (Figure 4). About 6% of uranium was associated with phase 1, represented by exchangeable cations and Ca carbonates and 4% related to the detrital material in the residual phase. Manganese oxides of nodules did not concentrate U, as was previously found by Och et al. [76].

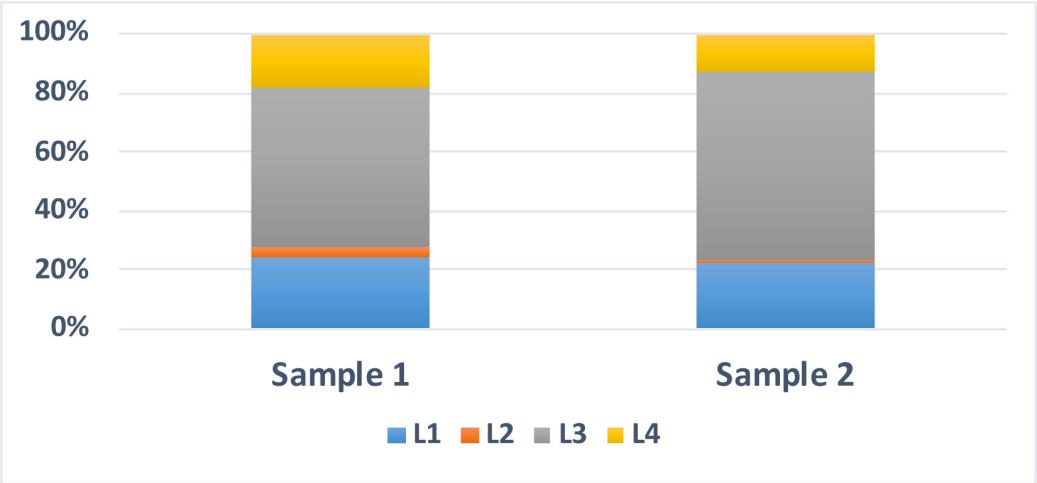

Figure 4. U distribution between four leaching steps in nodules from the Bolshoy Ushkany Island. Blank bars are analytical data with poor recovery through the leaching steps with respect to the bulk analyses, using a cutoff of 100% ± 20% recovery. Key: L1, exchangeable ions plus carbonate; L2, Mn-oxide; L3, Fe-oxyhydroxide; L4, residual fraction.

3.2.3. Age of Fe-Mn Nodules

Layer-by-layer ^{230}Th/U dating analyses of two Fe-Mn nodules included four and three measurements for each sample, with an analysis step of 2 mm (Table 1). The initial time of the sample 1 formation, which corresponds to the nodule inner layer, was approximately 131 ± 8 Ka. Sample 3 was slightly younger and showed 96 ± 5 Ka, which may be related to its location near the surface. The results indicate a high growth rate, which is characteristic of diagenetic deposits.

Table 1. Results of radiochemical analysis of the samples 1 and 3.

Samples	Study Layers (cm)	^{238}U dpm/g *	^{234}U dpm/g	^{230}Th dpm/g	^{232}Th dpm/g	^{230}Th/^{234}U	^{234}U/^{238}U	^{230}Th/^{232}Th	Age, Kyr
Sample 1	0.6–0.8	32.96 ± 0.59	38.54 ± 0.68	21.10 ± 0.52	1.27 ± 0.08	0.55 ± 0.02	1.17 ± 0.02	16.59 ± 1.05	88 ± 4
	0.4–0.6	21.28 ± 0.35	24.58 ± 0.40	17.64 ± 0.47	1.52 ± 0.09	0.72 ± 0.02	1.16 ± 0.01	11.64 ± 0.67	131 ± 8
	0.2–0.4	28.67 ± 0.69	34.43 ± 0.80	24.07 ± 0.68	1.44 ± 0.11	0.70 ± 0.03	1.20 ± 0.02	16.68 ± 1.26	124 ± 8
	0.0–0.2	35.95 ± 0.73	42.52 ± 0.84	29.28 ± 0.65	1.28 ± 0.08	0.69 ± 0.02	1.18 ± 0.02	22.93 ± 1.41	121 ± 7
Sample 3	0.4–0.6	31.93 ± 0.94	47.44 ± 1.34	27.69 ± 0.81	2.10 ± 0.11	0.58 ± 0.02	1.49 ± 0.03	13.20 ± 0.63	90 ± 5
	0.2–0.4	25.93 ± 0.64	39.32 ± 0.91	23.48 ± 0.60	2.05 ± 0.11	0.60 ± 0.02	1.52 ± 0.03	11.45 ± 0.56	92 ± 5
	0.0–0.2	24.50 ± 0.62	38.80 ± 0.91	23.84 ± 0.48	2.02 ± 0.09	0.61 ± 0.02	1.58 ± 0.03	11.79 ± 0.51	96 ± 5

* dpm/g = decays/min/g.

3.3. Microbial Communities

3.3.1. Alpha Diversity of Microbial Communities in the Sediments and Fe-Mn Nodules

Species richness (Chao1), and Shannon and Simpson diversity indices were normalized relative to the minimum number of reads, to compare alpha diversity in different layers of the sediments (Figure 5).

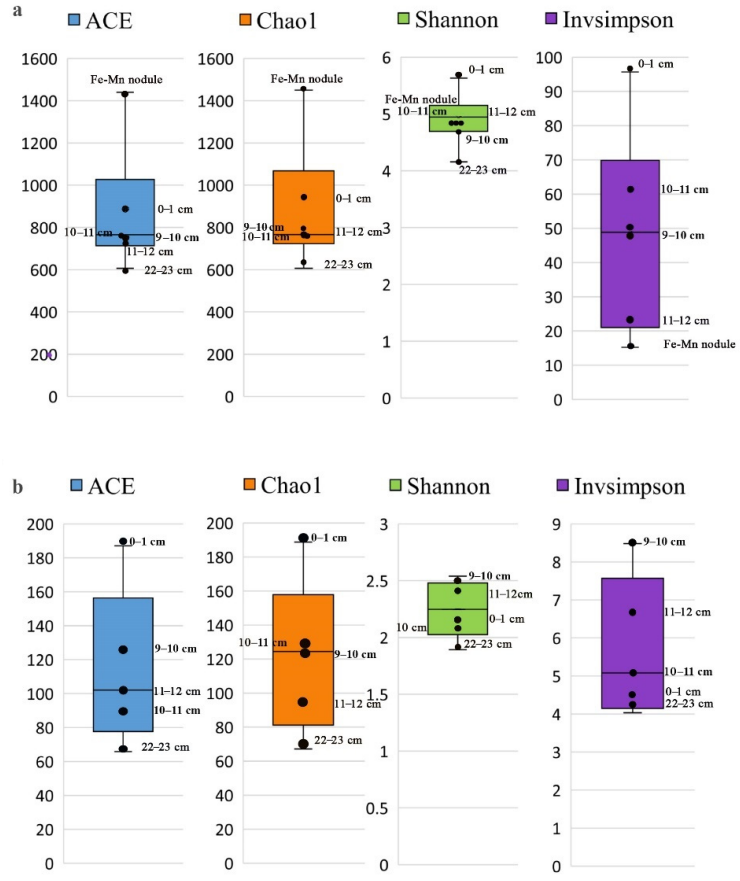

Figure 5. Box plots show (**a**) bacterial and (**b**) archaeal alpha diversity (ACE and Chao1 hidden richness estimators, Shannon Index and inverse Simpson Index); variation across samples from Bolshoy Ushkany Island based on non-rarefied data (for a cluster distance of 0.03).

Analysis of alpha diversity revealed that the highest indices among all sedimentary layers reflecting the hidden richness (ACE and Chao1), and richness and evenness (Shannon and Inverse Simpson) are typical for bacterial and archaeal communities from the surface layer (0–1 cm) (Figure 5; Supplementary Table S1). The taxonomic diversity of bacterial and archaeal communities decreases with the depth of the sediments. The bacterial community of Fe-Mn nodules had the highest species richness indices with the ACE and Chao of

1439 and 1450, respectively, and the Shannon and Inverse Simpson values were lower in comparison to the sediment communities (Figure 5).

3.3.2. Beta Diversity of Microbial Communities

Organoheterotrophic members of *Chloroflexi* (16–51%), *Acidobacteriota* (4.2–15%), *Actinobacteriota* (4.0–16.7%), and *Methylomirabilota* (5.2–13%) involving in AOM, significantly contribute to the bacterial communities of all the sedimentary layers studied (Figure 6a). The amount of phylum *Acidobacteriota* sequences, which is capable of phototrophy and iron reduction [77,78], was 4% in sample 22–23 cm (St6 Grf7) and was much higher in other samples (11–17%). They were also able to dissimilate inorganic and/or organic sulfur compounds [79]. The sequences of the phyla *Nitrospirota* and *Proteobacteria* (mainly *Gammaproteobacteria*) in the surface sediment community reach 9% and 15%, respectively (Figure 6a) and had a low content in the lower sedimentary layers (1–3%). Organoheterotrophic members of the order *Pseudomonadales* predominate among *Gammaproteobacteria*, and the sequences of the order *Nitrospirales*—among *Nitrospirota*. The taxa *Bacteroidota* and *Verrucomicrobiota* are widely spread in the sediments of Lake Baikal although they only existed in small amounts in all communities of the sediments studied and amount to 0.1 and 2.5%, respectively. Members of *Firmicutes* are also minor, the number of sequences was 3.5% in the 22–23 cm sample, decreasing by less than 1% in the upper layers. The sequences of *Verrucomicrobiota*, *Latescibacterota*, *Gemmatimonadota*, *Dadabecteria*, and RCP2-54 were less than 3% of reads in the communities (Figure 6b).

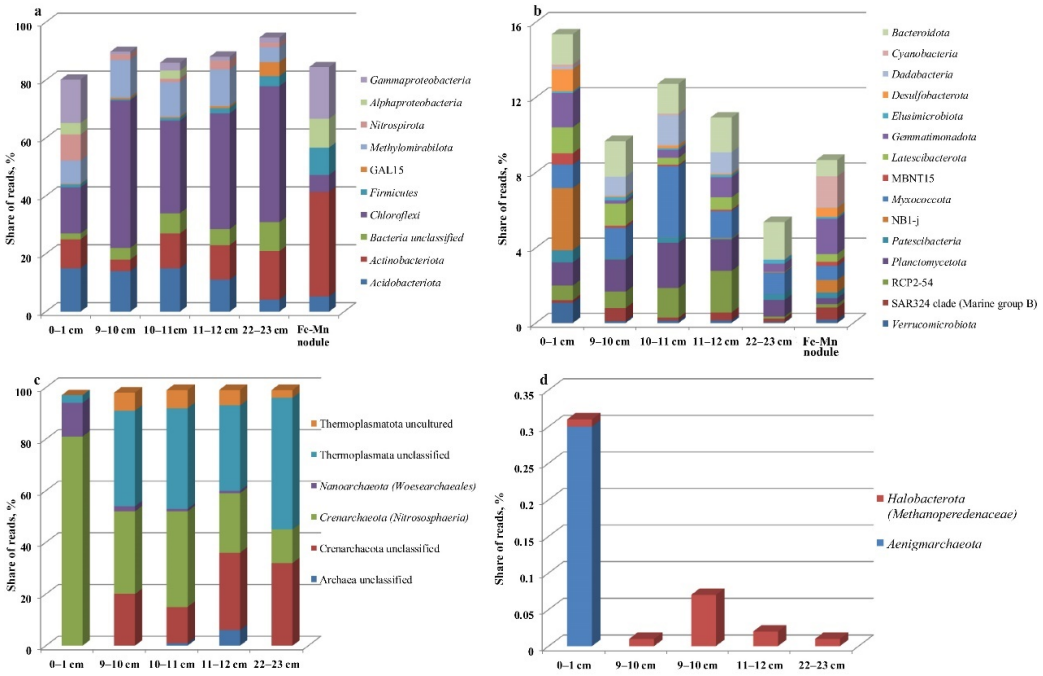

Figure 6. Taxonomic composition (**a**,**b**) of the bacterial and (**c**,**d**) archaeal communities in the bottom sediments near Bolshoy Ushkany Island, as well as in the Fe-Mn nodule at the phylum level; **a**,**c**—more than 97% of reads; (**b**,**d**)—less than 3% of reads.

The microbial community of the Fe-Mn nodule had a lower number of dominant phyla and a wide range of OTUs with a small number of sequences of different taxa (Figure 6a,b). The dominant phyla include *Actinobacteriota* (36.2%), *Firmicutes* (9.5%), *Chloroflexi* (5.8%), *Acidobacteriota* (5.3%), and classes *Alpha-* and *Gammaproteobacteria* (10 and 17.8%, respectively). Sequences of the phyla *Methylomirabilota* and *Nitrospirota* occurred in small amounts. The wide range of OTUs in the 16S rRNA gene library of the Fe-Mn nodule had a minor component of the community (less than 3% of reads less than 3% of reads of all bacterial 16S rRNA sequences; Figure 6b). They were most similar to those involved in the

destruction of substrates under aerobic and anaerobic conditions from different ecotopes, such as anaerobic chemoheterotrophic members of the candidate phylum *Acetothermia* that obtain energy and carbon by fermenting peptides, amino acids and simple sugars to acetate, formate and hydrogen [80]; anaerobic *Dehalococcoidia* (FS117-23B-02_ge, GIF9, MSBL5) that use halogenated compounds as electron acceptors [81] and occur in the communities of the sediments and deep water in the southern basin of Lake Baikal (personal data) [82]; and microarophillic Ca. Methylospira involved in methane oxidation, and others.

The comparison of beta diversity based on the Bray–Curtis distance matrix displayed the heterogeneity of the structure of bacterial communities at different depths of sediments and in comparison with Fe-Mn nodule (Figure 6a,b). The structure of the bacterial community in sample 22–23 cm differed from the others by the dominance of members of *Chloroflexi*, GAL15, *Firmicutes, Actinobacteriota*, and unclassified bacteria. Communities from other sediment layers had a more similar composition. They contained *Methylomirabilota* members and different contribution of dominant members of *Chloroflexi*, *Acidobacteriota* and *Actinobacteriota*.

Contribution to the bacteria of the phylum *Methylomirabilota* involved in the methane cycle is a varied. The number of sequences of this phylum in the communities of Fe-Mn nodules was less (2.4%) than in the communities of Fe-Mn layers (12–13%) and in sedimentary layers 0–1 cm and 22–23 cm (8.7% and 5.2%, respectively). Some order *Methylomirabilales* sequences of different OTUs formed one cluster in the phylogenetic tree and some OTU (Figure 7) groups with the sequences that we had previously detected in the sediments of methane seeped from the southern and central basins of Lake Baikal as well as in other ecosystems, including sediments of the freshwater Lake Constance. Members of *Rokubacteriales* (*Methylomirabilota*) order with mixotrophic metabolism that associated with nitrate respiration are more popular in the communities of Ushkanyi sediments [83]. The sequences from volcanic and manganese deposits and from soil and freshwater ecosystems were identified among the closest homologues.

The taxonomic composition of the archaea was obtained only in sediments (Figure 6c,d). Archaeal communities were less diverse in comparison to bacterial ones, which is typical for benthic microbial communities of Lake Baikal [84]. The surface sediment community contained predominantly ammonium-oxidizing archaea of the class *Nitrososphaeria* (*Crenarchaeota*) (81.6%) and a lower amount of the phylum *Nanoarchaeota* sequences (13.5%) (order *Woesearchaeales*) and the unclassified *Thermoplasmata* (3.8%). The community of lower sedimentary layers consisted of the class *Nitrososphaeria* (45.6–53.1%) and the unclassified *Thermoplasmata* (39.4–54.0%), which increased significantly. The unclassified archaea grew in the community of sample 11–12 cm (6.3%), while members of *Nanoarchaeota* (0.3–2.1%) decreased in the community of the anaerobic zone. Phylogenetic analysis of *Woesearchaeales* (Figure 8) revealed a predominance of nucleotide sequences of two OTUs (16 and 17) in the surface layer related to sequences from deep-sea ferromanganese in the western Pacific (unpublished data) and iron-silica-rich microbial mats in deep-sea crusts hydrothermal fields (Figure 8). Sample 9–10 cm showed high concentrations of Mn ions and its community contained sequences another OTU (34) also belonging to the order *Woesearchaeales.*

Methylotrophic methanogens of *Methanomassiliicoccales* of the phylum *Thermoplasmatota* (formerly *Euryarchaeota*) are depleted in three upper core communities (0.05–0.4%) and were not detected in the lower layers (11–12 cm and 22–23 cm). In the phylogenetic tree, the sequences of this order were combined with the closest homologue from the hypersaline microbial mat into one OTU (22) (Figure 8). The sequences of other groups of methanogenic archaea that provide hydrogenotrophic and acetoclastic methanogenesis were not observed; this was also the case during the previous study of archaeal communities in Fe-Mn layers of the southern basin with a slow sedimentation rate [49]. The class *Nitrososphaeria* members of the phylum *Crenarchaeota* (formerly *Thaumarhaeota*) predominated, which is common for the communities of Baikal surface sediments [85]. Among members of this class, we detected archaea of the orders *Nitrosopumilales* and *Nitrososphaerales*, known as participants in the aerobic oxidation of ammonium [86]. The number of order members decreased

with the sediment depth, caused most likely by the lack of oxygen necessary for their development. Presumably, *Nitrososphaeria* obtained energy from ammonium oxidation and carried out not only autotrophic metabolism but also heterotrophic metabolism [87]. The homologues of samples 0–1 cm and 9–10 cm, which are the closest to the uncultivated sequences of *Nitrososphaeria*, were identified in Fe-Mn sediments and Mn nodules [88]. In the phylogenetic tree, the sequences of some OTUs formed separate clusters or separate branches with uncultivated members of this taxon. The tree topology of the taxon based on the analysis of 16S rRNA gene fragments of individual OTUs was similar to the topology of the tree (Figure 8) that was previously obtained in areas of mineralized fluid discharge by using the other platform (Roshe 454) [49,89].

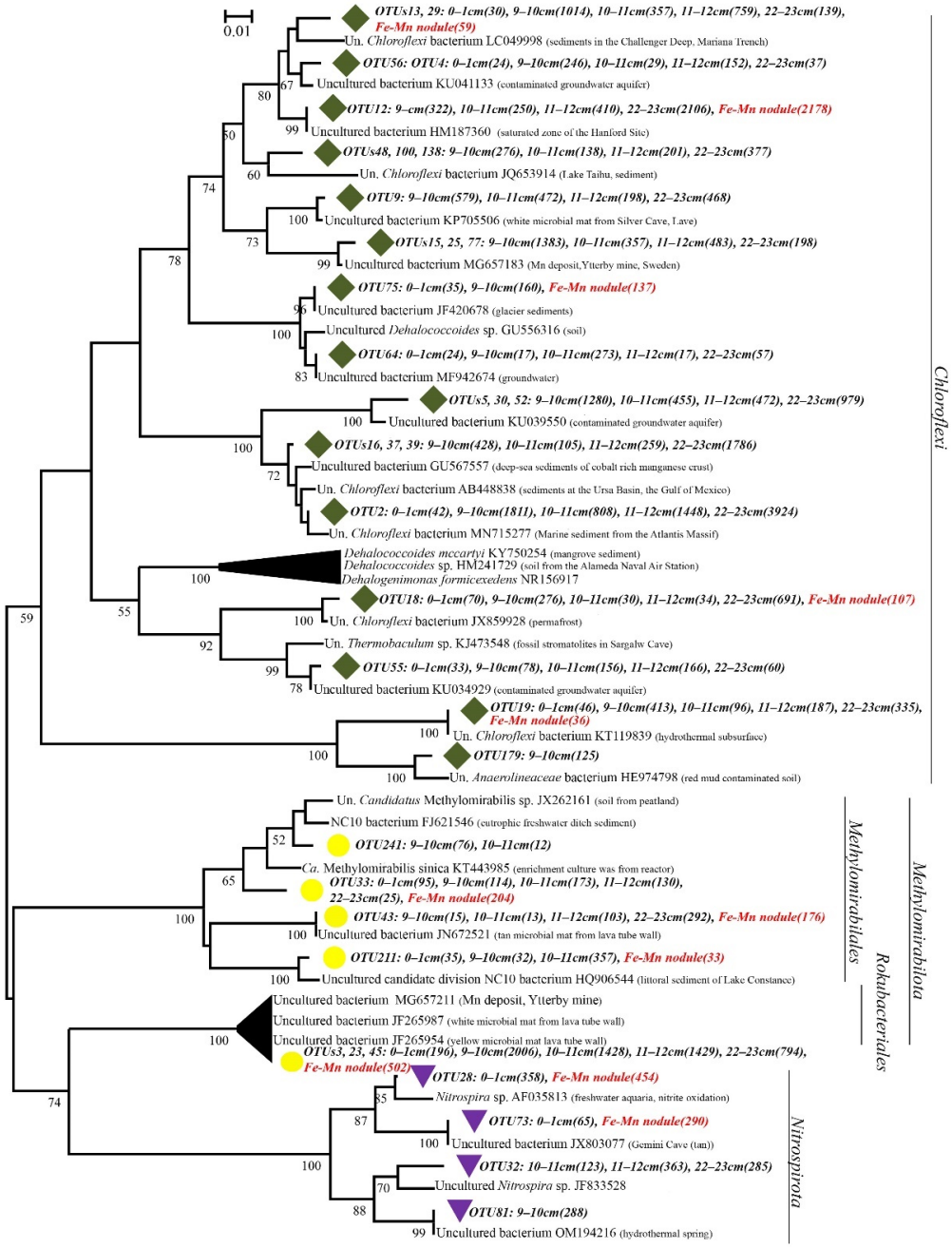

Figure 7. Neighbor-joining (NJ) phylogenetic tree of dominant phyla based on 16S rRNA gene sequences of phyla *Methylomirabilota*, *Nitrospirota*, and *Chloroflexi*. Bootstrap values > 50% (of 100 replicates) are shown in front of respective nodes, and the scale bar represents 5% sequence divergence. OTUs described in this work is represented by circles, lozenges, and upside triangles.

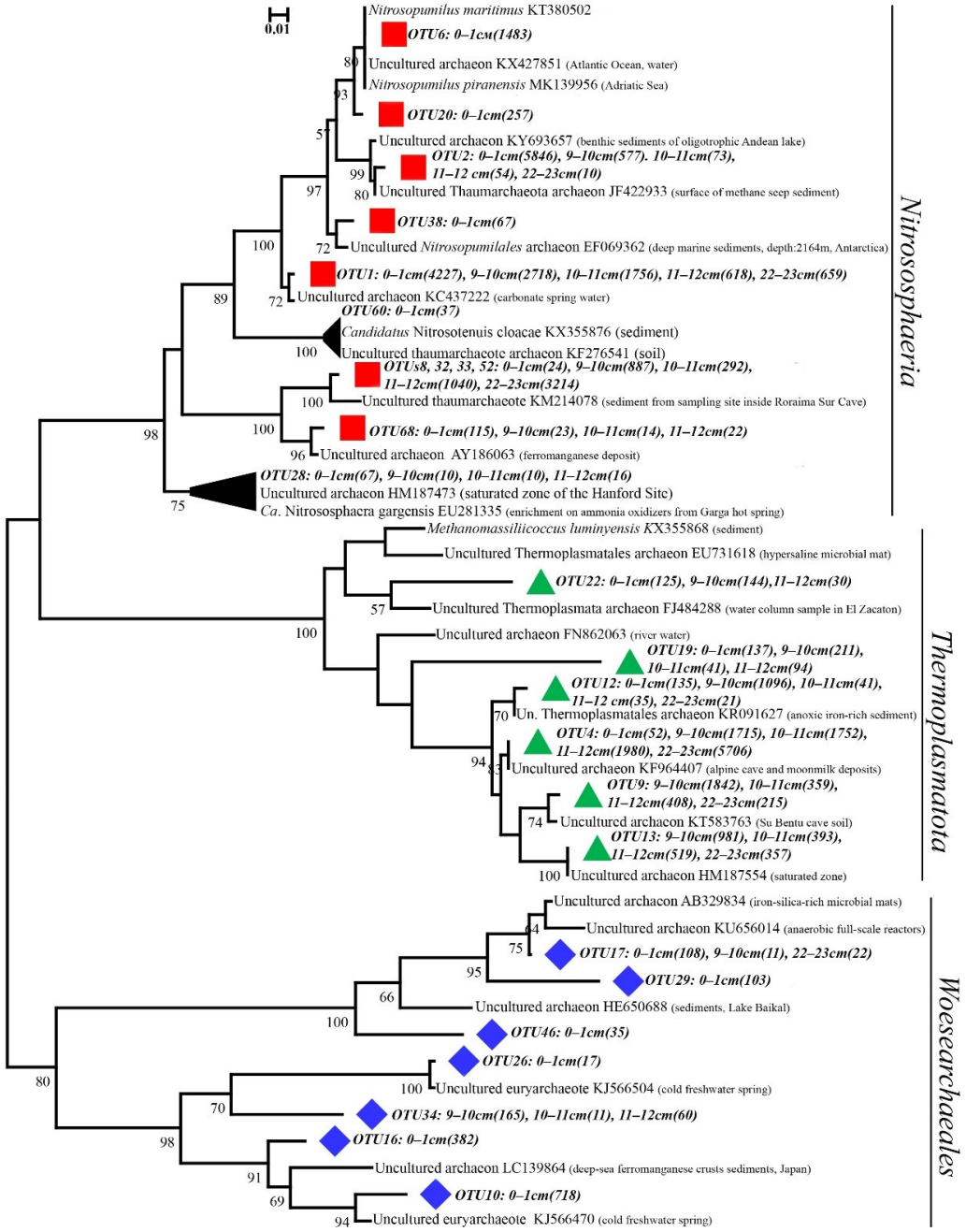

Figure 8. NJ phylogenetic tree of dominant phyla based on 16S rRNA gene sequences of class *Nitrososphaeria* (*Crenarchaeota*), order *Woesearchaeales* and phylum *Thermaplasmatota*. Bootstrap values > 50% (of 100 replicates) are shown in front of respective nodes, and the scale bar represents 5% sequence divergence. OTUs described in this work are represented by squares, lozenges, and triangles.

3.4. Community Analysis

Venn diagrams revealed general and unique OTUs for each analyzed community (Figure S2). The largest number of unique OTUs were in the 16S rRNA gene library of the Fe-Mn nodule, including sequences that were identical to bacteria from different ecotopes. The contribution of OTUs with the abundance of 0.5% in the communities of Fe-Mn sedimentary layers and the Fe-Mn nodule was assessed (Figure 9). Fe-Mn nodule community predominantly had OTUs of unclassified members of different taxa, which complicated the assessment of their metabolism and participation in Fe and Mn cycling.

Nevertheless, the Fe-Mn nodule community contained sequences of the genus *Pedomicrobium*, the cultivated members of which are involved in Fe cycling [90], and uncultivated members of *Alphaproteobacteria*, some of which predominate in hydrogenetic crusts [91,92]. Genomic studies of Ca. Kryptonia confirmed the capacity of iron to redox transformation under thermophilic conditions. The Ca. Kryptonia sequences were more numerous in the communities of the sediments. The members of the genus *Delftia* and *Sulfurifustis* that participate in the immobilization of heavy metals and are typical of thermophilic ecotopes minor OTUs (<0.5%) occurred in the community of the Fe-Mn nodule [93,94]. These sequences were similar to thermophilic green non-sulfur bacteria (*Thermomicrobiales* AKYG1722), *Thermodesulfovibrionia* (*Nitrospirota*) involved in the nitrogen cycle [95]; thermophilic thiosulfate-reducing bacteria of the genus *Caldisericum* (*Caldisericota*) [96]; aerobic *Tumebacillus* from hot spring [97], and bacteria of the *Planifilum* df genus of the *Thermoactinomycetales* family (*Firmicutes*).

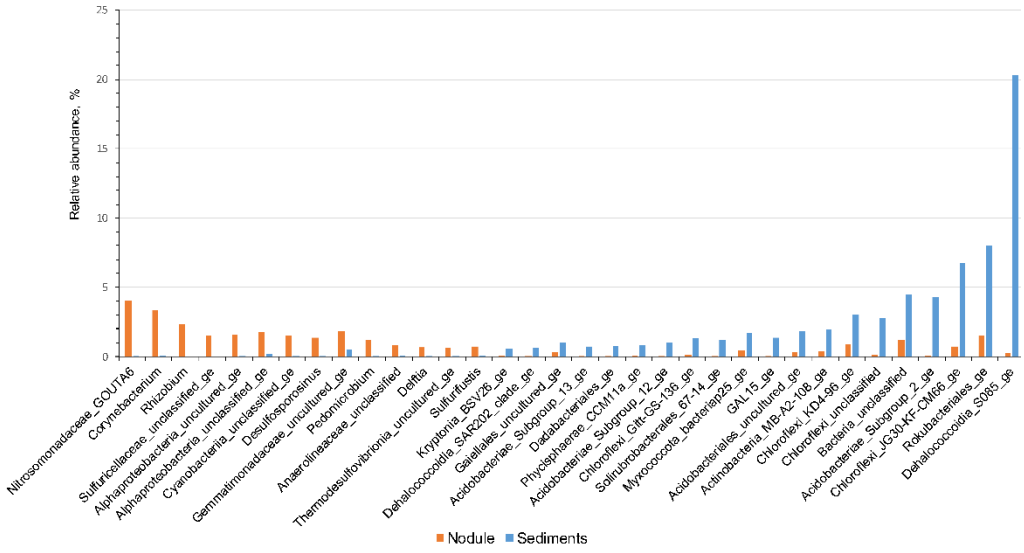

Figure 9. $OTUs_{0.03}$ with relative abundance > 0.5% (on average for sediments and in absolute values for the nodule) and difference in relative abundance between the nodule and sediments by a factor of three or more.

The members of *Chloroflexi* with a wide habitat are the most typical for communities of sediments. They were observed in underground environments, in communities of subsurface sediments [98] including iron-rich hot springs [99]. Many members of this phylum occur in the microbial communities of the studied Fe-Mn layers and Fe-Mn nodules, forming several clusters from different ecosystems with the closest homologues in the phylogenetic tree (Figure 7). Uncultivated members of *Chloroflexi* (lineages S085_ge, KD4-96_ge, JG30-KF-CM66_ge) and members of the order *Rokubacteriales* (*Methylomirabilota*) exist in the communities of Fe-Mn layers and Fe-Mn nodules (Figure 9).

The results of the interaction of bacterial and archaeal taxa (positive or negative) with chemical parameters of the habitat (Spearman correlation) are shown as a heat map (Figure 10a,b). Both were divided into two clusters with a small number of significant correlations between individual taxa of bacteria and the ions concentration in the pore water. Thus, members of *Methylomirabilota* and *Nitrospirota* positively correlated with SO_4^{2-} with a high degree of significance ($p_v < 0.05$); *Actinobacteriota*—with K^+ and Na^+; *Firmicutes*—with NO_3^-, K^+ and Na^+ and *Alphaproteobacteria*—with NO_2^-. Significant negative correlation existed between unclassified bacteria members and NO_2^-. The individual ions with various archaeal taxa also showed both positive and negative correlation (Figure 10b). Members of *Nitrososphaeria* (*Crenarchaeota*) positively correlated ($p_v < 0.05$) with the SO_4^{2-} and negatively correlated with K^+. By contrast, unclassified members of the same phylum showed a positive correlation with K^+ and a negative correlation with SO_4^{2-}. There were

negative relationships between K^+, Na^+ and Mn^{2+} ions and the sequences of *Woesearchaeales* and positive ones between members of *Thermoplasmata* and Mn^{2+} as well as between unclassified *Archaea* and Fe^{2+}.

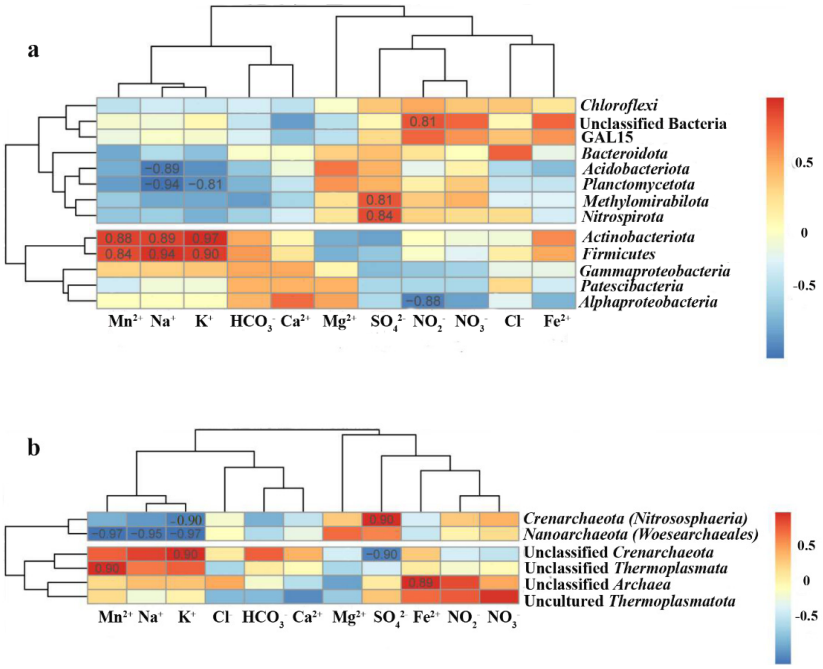

Figure 10. Heat map of correlation relationships (Spearman correlation) between (**a**) bacterial/(**b**) archaeal taxa and the concentration of individual ions in the pore water of the investigated bottom sediments. Different colors indicate correlation coefficients based on the color scale to the right of the heat map. The coefficients $p_v < 0.05$ are shown.

4. Discussion

Fe-Mn sediment layers and Fe-Mn nodules occurred on the northern slope of Bolshoy Ushkany Island at a depth of 650 m within the first metre of sediments. The results coincided with the PISCES submarine discovery of Fe-Mn mineralization at the depth of 450–510 m on the same slope [50]. The lithology of the sediments studied (Figure 2a) corresponds to areas with calm sedimentation [100,101] but with the narrower boundaries of Holocene sediments (diatom ooze M1 (0–~11 Ka)). The age of Fe-Mn nodules collected from the Holocene sediments indicated their earlier formation with the initial age of accumulation as 131 ± 8 Ka and 96 ± 5 Ka, as well as the conditions for their preservation up to the present day. Many scientists agree that the preferential concentration of nodules at and near the sediment surface is due to the activity of benthic organisms, which can slightly move the nodules and not allow sediments to cover them [102]. Another explanation of the Fe-Mn nodule existence in the more recent Holocene sediments is the landslide processes that have partly occurred in the area, and which were previously shown using the PISES submarines [50]. Landslide processes at the slope might also have influenced the diagenesis processes and the structure of microbial communities. The most significant changes in the structure of microbial communities of area studied were observed between oxidized and reduced conditions, as in other freshwater lakes such as Lake Stechlin and five lakes in Central Switzerland [103,104]. The contribution of *Verrucomicrobiota* and *Bacteroidota* members are decreased, and representatives of phyla *Chloroflexi*, *Methylomirabilota* are increased in this samples. Ammonium-oxidizing archaea of the *Nitrososphaeria* (*Crenarchaeota*) class comprised more than 80% in the sediment communities, which may reflect the availability of ammonium in the sediments studied. It is consistent with the diversity of the communities of Fe-Mn deposits from RGR [9], where bacterial and archaeal groups are associated with the oxidation of nitrogen compounds (such as *Nitrospirota, Nitrospinota* and *Nitrosopumilus)* and are involved in methane oxidation (i.e., *Methylomirabilales*

(*Methylomirabilota*) and SAR324 (*Deltaproteobacteria*)). Chemolithoautotrophs, which were related to ammonium-oxidizing archaea and nitrite-oxidizing bacteria, can potentially play a very important role as primary producers of Fe-Mn deposits [9]. *Thaumarchaeota* (now *Nitrososphaeria*) members may be involved in manganese oxidation due to presence of multicopper oxidase in their genomes [105]. Therefore, the chemolithoautotrophic bacteria, ammonia-oxidizing archaea (*Nitrososphaeria*), and *Methylomirabilota* bacteria using nitrite ion as electron acceptor dominated in the sedimentary Fe-Mn layers in deep-water Baikal and Bolshoy Ushkany Island. Based on the genome investigations, *Acidobacteriota* members can participate in the iron cycle [106], although cultural studies of only *B. elongata* species confirmed this capacity [38]. The dominance of phylogenetically diverse chemoautotrophs such as *Chloroflexi* and *Actinobacteriota* does not exclude their active role in the formation of organic matter, which is required for the community activity in general [107]. Members of *Alphaproteobacteria* and *Gammaproteobacteria*, in particular *Alteromonadales*, prevailed in bacterial communities of Fe-Mn deposits from the CCZ of the North Pacific Ocean [107]. Furthermore, members of *Bacteroidota, Actinobacteriota, Planctomycetota*, and *Verrucomicrobiota* often occur in the community of CCZ nodules and reach approximately from 1 to 10% of the total abundance [107]. We indicated a minor contribution of *Verrucomicrobiota, Latescibacterota, Gemmatimonadota, Dadabecteria* and RCP2-54 members in the communities of the core studied, but their role in Fe-Mn layers formation is not obvious.

The dynamic growth of Fe and Mn initiates immediately under the layer of maximum O_2 penetration and the dissolution of particulate Fe and Mn is caused by AOM or sulfate reduction (SO_4^{2-}) and subsequent formation of Fe(II) via S(II) oxidation, or is directly associated with Fe reduction Och et al. [29]. An alternative process of Fe(II) dissolution by anaerobic NH_4^+ nitrification was proposed by Torres et al. [108]. As mentioned above, the sequences of microorganisms of the nitrogen cycle, including ammonium oxidizing archaea (*Nitrososphaeria*), *Woesearchaeales* and the *Nitrosomonadaceae* bacteria in the communities of the sediments studied are the most diverse. They can provide denitrification processes and dissimilatory reduction of nitrates to ammonium and be involved in the chain of trophic interactions with anaerobic methanotrophs. Genomic studies of anaerobic enzymatic heterotrophs of the order *Woesearchaeales* also display their capacity to participate in iron metabolism and methanogenesis processes [109] in consortium with methanogens [30]. Sequences of methylotrophic methanogens of the order *Methanomassiliicoccales* occurred in three communities (0–1 cm, 9–10 cm and 10–11 cm), but the methane concentrations of sediments did not confirm their activity. A comparative genomic analysis and ecological distribution of archaea of this taxon also suggested their possible participation in the denitrification processes, nitrogen fixation and dissimilatory nitrite reduction [110]. The contribution of archaea that use other metabolic ways to produce methane was insignificant, raising doubts about their active role in the Mn and Fe cycles in the sediments studied. The bacteria of the phylum *Methylomirabilota* participating in nitrite dependent AOM [85] represented anaerobic methanotrophs in the microbial communities analyzed. Sequences of the order *Rokubacteriales,* having mixotrophic metabolism associated with nitrogen respiration, predominated among them [83]. The dissolution of particulate Fe and Mn in the studied sediments most likely occurred due to anaerobic nitrification of NH_4^+ and nitrate dependent AOM, which corresponds to the assumption of Torres et al. [108], rather than due to sulfate reduction [29]. The reduction of iron with sulfur using anoxygenic phototrophs is also unlikely, due to the great depth of the area studied, although the process is typical for some freshwater lakes [111–113]. Analysis of 16S rRNA gene libraries did not reveal typical phototrophic iron-oxidizing and sulfate-oxidizing bacteria, whereas a small amount of the latter was observed in Fe-Mn nodules and the surface sedimentary layer. It is also possible that high Mn and low Fe(II) content in sediments at a depth of 22–23 cm did not provide the reductive dissolution of its oxides by Fe(II) [29] and their migration into the upper sedimentary layers.

The Fe-Mn nodules studied differ from those of the deep-ocean and southern Baikal by the predominance of iron over manganese [5,114]. Fe-Mn nodules sampled at a depth of

27 cm have a Mn/Fe ratio of 0.13, and those near the redox boundary is 0.33. The differences in Mn/Fe ratio might reflect the burial process and remobilization of iron and manganese layers in the sediments, which are described in Och et al. [29]. REY distribution was a useful tool for studying Fe-Mn deposits genesis. Nodules studied showed negative Ce anomaly, which is typical for diagenetic deposit distribution of REY normalized to PAAS (Figure 11a,b). The porewaters were not able to reduce or transport $Ce^{4+,}$ therefore sub-oxic porewaters mobilized Mn^{2+} and REY^{3+} while Ce^{4+} remained fixed in discrete Ce (IV) compounds [17]. Due to the subsequent oxidation of divalent Mn and the formation of diagenetic nodules, Ce was not quantitatively mobilized. Hydrothermal type also has a negative Ce anomaly and a positive Y anomaly, which, however, is typical only for hydrothermal fluids with temperatures above 200 °C [17]. On the bivariate diagram of Ce_{SN}/Ce_{SN}* ratio vs. Nd concentration, the samples plot in the diagenetic nodules field (Figure 11c), confirming the assumption about the predominant diagenetic formation of nodules from pore water [17]. Samples at the Ce_{SN}/Ce_{SN}* ratio vs. $Y_{SN}/Ho_{SN,}$ located on the boundary of diagenetic and hydrothermal deposit fields, reflected a Y_{SN}/Ho_{SN} ratio of approximate 1 (Figure 11d), coinciding with the Y_{SN}/Ho_{SN} ratio of porewater from the Bering Sea Slope (mean 1.07) [115]. Hydrothermal Fe–Mn deposits can trend towards hydrogenetic Fe–Mn crusts in plots of the Ce_{SN}/Ce_{SN}* vs. Y_{SN}/Ho_{SN} ratio and Ce_{SN}/Ce_{SN}* vs. Nd concentration [17], which supports the assumption of a hydrothermal influence, in particular, an additional supply to pore waters in the area of diagenetic formation of nodules. The influence of low-temperature hydrothermal activity was also observed in films on rock fragments collected from the Ushkani island slope [50]. The hydrothermal influence may explain the higher diversity of the bacterial community in the Fe-Mn nodules compared to the diversity in the sediment, including the Fe-Mn layers, and the presence of a wide range of minor OTUs closely related to the inhabitants of geothermal ecotopes.

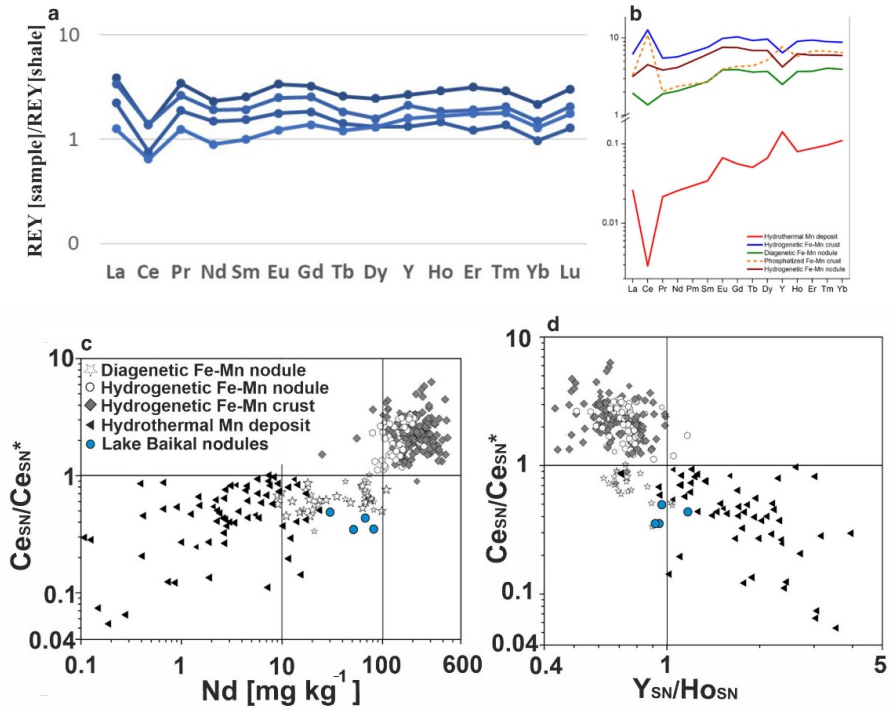

Figure 11. (**a**) Distribution of REY normalized to PAAS of Fe-Mn nodules from Ushkani islands; (**b**) Examples of typical REY patterns of marine hydrothermal Fe and Mn deposits, diagenetic Fe–Mn nodules, hydrogenetic Fe–Mn nodules, hydrogenetic Fe–Mn crusts, and phosphatized hydrogenetic Fe–Mn crusts; Marine Fe–Mn oxyhydroxide deposits for (**c**) Ce_{SN}/Ce_{SN}* vs. Nd concentration and (**d**) Ce_{SN}/Ce_{SN}* ratio vs. Y_{SN}/Ho_{SN} (Bau et al., 2014); SN is shale normalized to Post-Archean Australian Shale, PAAS (McLennan, 1989); Ce* = Ce anomaly (Ce_{SN}* = 0.5La_{SN} + 0.5 Pr_{SN}).

According to Colman et al. [100] and Vologina et al. [101], the age of the sediments studied is about 10,000–12,000 years, which is younger than the Fe-Mn nodules. The DNA from microorganisms, which are involved in diagenetic processes, and those from sediments presumably precipitate for a long time on the surface or inside the Fe-Mn nodules and have been preserved until now. Therefore, it is most likely that the bacterial diversity of Fe-Mn nodules reflects the communities of the area studied for a period of 100 Ka. The hypothesis presented here will have to be tested through a more thorough sampling of Fe-Mn nodules from different depths of sediments, as well as through studies of isotopic composition and composition of microbial communities in nodules from different depths.

Our results show that the composition of microbial communities of Fe-Mn sedimentary layers differed from those of surface sediments and Fe-Mn nodules. Bacterial and archaeal groups associated with the oxidation of nitrogen and methane compounds mainly dominated the communities of Fe-Mn layers. Chemolithoautotrophs that are associated with ammonia-oxidizing archaea and nitrite-oxidizing bacteria can potentially play an important role as primary producers of Fe-Mn substrates in freshwater Lake Baikal, which is similar in marine ecotopes. However, the above results are not final because the diversity of microbial communities from Fe-Mn deposits also clearly demonstrates an individual variability in different areas of Lake Baikal as well as in the World Ocean [9,21,49,105]. Nevertheless, the data obtained expanded our knowledge about the diversity and structure of microbial communities as well as their potential role as possible participants of dissolution/formation of the buried Fe-Mn oxide layer in the deep-water Lake Baikal.

Supplementary Materials: The following supporting information can be downloaded at: https://www.mdpi.com/article/10.3390/d14100868/s1, Figure S1: Heat map showing the differences in the relative abundance of phyla (classes) in the samples, leading to the formation of two clusters (average linkage clustering) based on the Bray-Curtis distances. The colors mark the normalized relative abundance of taxa across all stations; Figure S2: Venn diagram revealed both general and unique OTUs for each analyzed communities; Table S1: Number of reads, OTUs and indices of species hidden richness and evenness in the non-rarefied libraries of bacterial and archaeal 16S rRNA gene fragments (for a cluster distance of 0.03).

Author Contributions: Conceptualization, T.Z., N.K. and A.L.; methodology, N.K., O.K., O.S. and S.B.; formal analysis, S.B., T.P., A.L., O.K., A.K. and V.I.; investigation, O.S., T.P., O.K., G.V. and V.I.; data curation, N.K, and T.Z.; writing—original draft preparation, T.Z. and N.K.; writing—review and editing, T.Z., A.L. and N.K.; visualization, A.K. and G.V.; project administration, T.Z. All authors have read and agreed to the published version of the manuscript.

Funding: The study of the chemical composition of Fe-Mn crusts was supported by the RSF grant No 18-17-00015; analyses of the chemical composition of pore water, of the diversity and structure of microbial communities by the State Project FWSR 0279-2021-0006.

Institutional Review Board Statement: Not applicable.

Informed Consent Statement: Not applicable.

Data Availability Statement: The BioProject accession number for these SRA data is: PRJNA875570; https://www.ncbi.nlm.nih.gov/sra/?term=PRJNA875570, accessed on 31 August 2022.

Acknowledgments: This study was carried out using the equipment of the Core Centrum "Genomic Technologies, Proteomics and Cell Biology" in ARRIAM. The authors would like to thank Irkutsk Supercomputer Center SB RAS for providing access to HPCcluster "Akademik V.M. Matrosov".

Conflicts of Interest: The authors declare no conflict of interest.

References

1. Baturin, G. *Geochemistry of Manganese and Manganese Nodules in the Ocean*; Reidel, D., Ed.; Springer: Dordrecht, Netherlands, 1988; p. 342. [CrossRef]
2. Baturin, G.; Yushina, I.; Zolotykh, E. Variations in the elemental composition of ferromanganese structures from Lake Baikal. *Oceanology* **2009**, *49*, 505–514. (In Russian) [CrossRef]

3. Baturin, G. Distribution of elements in ferrum-manganese nodules in seas and lakes. *Lithol. Miner.* **2019**, *5*, 404–417. (In Russian) [CrossRef]
4. Hayles, S.; Al, T.; Cornett, J.; Harrison, A.; Zhao, J. Growth rates for freshwater ferromanganese concretions indicate regional climate change in eastern Canada at the Northgrippian-Meghalayan boundary. *Holocene* **2021**, *31*, 1250–1263. [CrossRef] [PubMed]
5. Hein, J.R.; Koschinsky, A. Deep-ocean ferromanganese crusts and nodules. In *Treatise on Geochemistry*, 2nd ed.; Holland, H.D., Turekian, K.K., Eds.; Elsevier: Oxford, UK, 2014; Volume 13, pp. 273–291, Chapter 11.
6. Kholodov, V.N.; Nedumov, R.I.; Golubovskaya, E.V. Facies types of sedimentary iron ore deposits and their geochemical features: Communication 1. Facies groups of sedimentary ores, their lithology, and genesis. *Lithol. Miner. Resour.* **2012**, *47*, 447–472. [CrossRef]
7. Konstantinova, N.; Cherkashov, G.; Hein, J.R.; Mirão, J.; Dias, L.; Madureira, P.; Kuznetsov, V. Composition and characteristics of the ferromanganese crusts from the western Arctic Ocean. *Ore Geol. Rev.* **2017**, *87*, 88–99. [CrossRef]
8. Vereshchagin, O.S.; Perova, E.N.; Brusnitsyn, A.I.; Ershova, V.B.; Khudoley, A.K.; Shilovskikh, V.V.; Molchanova, E.V. Ferromanganese nodules from the Kara Sea: Mineralogy, geochemistry and genesis. *Ore Geol. Rev.* **2019**, *106*, 192–204. [CrossRef]
9. Bergo, N.M.; Bendia, A.G.; Neiva Ferreira, J.C.; Murton, B.J.; Brandini, F.P.; Pellizari, V.H. Microbial diversity of deep-sea ferromanganese crust field in the rio Grande Rise, Southwestern Atlantic Ocean. *Microb. Ecol.* **2021**, *82*, 344–355. [CrossRef]
10. Emerson, D.; Field, E.K.; Chertkov, O.; Davenport, K.W.; Goodwin, L.; Munk, C.; Nolan, M.; Woyke, T. Comparative genomics of freshwater Fe-oxidizing bacteria: Implications for physiology, ecology, and systematic. *Front. Microbiol.* **2013**, *4*, 254. [CrossRef]
11. González, F.J.; Rincón-Tomás, B.; Somoza, L.; Santofimia, E.; Medialdea, T.; Madureira, P.; López-Pamo, E.; Hein, J.R.; Marino, E.; de Ignacio, C.; et al. Low-temperature, shallow-water hydrothermal vent mineralization following the recent submarine eruption of Tagoro volcano (El Hierro, Canary Islands). *Mar. Geol.* **2020**, *430*, 106333. [CrossRef]
12. Kato, S.; Okumura, T.; Uematsu, K.; Hirai, M.; Iijima, K.; Usui, A.; Suzuki, K. Heterogeneity of microbial communities on deep-sea ferromanganese crusts in the Takuyo-Daigo seamount. *Microbes Environ.* **2018**, *33*, 366–377. [CrossRef]
13. Kato, S.; Hirai, M.; Ohkuma, M.; Suzuki, K. Microbial metabolisms in an abyssal ferromanganese crust from the Takuyo-Daigo Seamount as revealed by metagenomics. *PloS ONE* **2019**, *14*, e0224888. [CrossRef] [PubMed]
14. Jianga, X.-D.; Sun, X.-M.; Yao, G. Biogenic mineralization in the ferromanganese nodules and crusts from the South China Sea. *J. Asian Earth Sci.* **2019**, *171*, 46–59. [CrossRef]
15. Wang, X.H.; Schlossmacher, U.; Natalio, F.; Schröder, H.C.; Wolf, S.E.; Tremel, W.; Müller, W.E. Evidence for biogenic processes during formation of ferromanganese crusts from the Pacific Ocean: Implications of biologically induced mineralization. *Micron* **2009**, *40*, 526–535. [CrossRef] [PubMed]
16. Wang, X.; Muller, W.E.G. Marine biominerals: Perspectives and challenges for polymetallic nodules and crusts. *Trends Biotechnol.* **2009**, *27*, 375–383. [CrossRef]
17. Bau, M.; Schmidt, K.; Koschinsky, A.; Hein, J.R.; Kuhn, T.; Usui, A. Discriminating between different genetic types of marine ferro-manganese crusts and nodules based on rare earth elements and yttrium. *Chem. Geol.* **2014**, *381*, 1–9. [CrossRef]
18. Hein, J.R.; Koschinsky, A.; Halbach, P.E.; Manheim, F.T.; Bau, M.; Kang, J.; Lubick, N. Iron and manganese oxide mineralization in the Pacific. *Geol. Soc. Spec. Publ.* **1997**, *119*, 123–138. [CrossRef]
19. Hein, J.R.; Koschinsky, A.; Bau, M.; Manheim, F.T.; Kang, J.-K.; Roberts, L. Cobalt-rich ferromanganese crusts in the Pacific. In *Handbook of Marine Mineral Deposits*; Cronan, D.S., Ed.; CRC Press: Boca Raton, FL, USA, 1999; pp. 239–279.
20. Orcutt, B.N.; Bradley, J.A.; Brazelton, W.J.; Estes, E.R.; Goordial, J.M.; Huber, J.A.; Jones, R.M.; Mahmoudi, N.; Marlow, J.J.; Murdock, S.; et al. Impacts of deep-sea mining on microbial ecosystem services. *Limnol. Oceanogr.* **2020**, *65*, 1489–1510. [CrossRef]
21. Molari, M.; Janssen, F.; Vonnahme, T.; Wenzhöfer, F.; Boetius, A. The contribution of microbial communities in polymetallic nodules to the diversity of the deep-sea microbiome of the Peru Basin (4130–4198 m depth). *Biogeosciences* **2020**, *17*, 3203–3222. [CrossRef]
22. Strakhovenko, V.; Subetto, D.; Ovdina, E.; Belkina, N.; Efremenko, N. Distribution of elements in iron-manganese formations in bottom sediments of Lake Onego (NW Russia) and small lakes (Shotozero and Surgubskoe) of Adjacent Territories. *Minerals* **2020**, *10*, 440. [CrossRef]
23. Zhang, G.-Y.; Zhang, L.-M.; He, J.-Z.; Liu, F. Comparison of archaeal populations in soil and their encapsulated iron-manganese nodules in four locations spanning from North to South China. *Geomicrobiol. J.* **2017**, *34*, 811–822. [CrossRef]
24. Hein, J.R.; Mizell, K.; Koschinsky, A.; Conrad, T.A. Deep-ocean mineral deposits as a source of critical metals for high-and green-technology applications: Comparison with land-based resources. *Ore Geol. Rev.* **2013**, *51*, R713–R715. [CrossRef]
25. Baturin, G.N.; Dubinchuk, V.T.; Novigatsky, A.N. Phase distribution of elements in ferromanganese nodules of the Kara Sea. *Dokl. Earth Sci.* **2016**, *471*, 1199–1203. (In Russian) [CrossRef]
26. Zhong, Y.; Chen, Z.; González, F.J.; Hein, J.R.; Zheng, X.; Li, G.; Luo, Y.; Mo, A.; Tian, Y.; Wang, S. Composition and genesis of ferromanganese deposits from the northern South China Sea. *J. Asian Earth Sci.* **2017**, *138*, 110–128. [CrossRef]
27. Edgington, D.N.; Callender, E. Minor element geochemistry of Lake Michigan ferromanganese nodules. *Earth Planet. Sci. Lett.* **1970**, *8*, 97–100. [CrossRef]
28. Moore, W.S.; Dean, W.E.; Krishnaswami, S.; Borole, D.V. Growth rates of manganese nodules in Oneida Lake, New York. *Earth Planet. Sci. Lett.* **1980**, *46*, 191–200. [CrossRef]
29. Och, L.M.; Müller, B.; Voegelin, A.; Ulrich, A.; Göttlicher, J.; Steiniger, R.; Mangold, S.; Vologina, E.G.; Sturm, M. New insights into the formation and burial of Fe/Mn accumulations in Lake Baikal sediments. *Chem. Geol.* **2012**, *330–331*, 244–259. [CrossRef]

30. Liu, Q.; Huo, Y.Y.; Wu, Y.H.; Bai, Y.; Yuan, Y.; Chen, M.; Xu, D.; Wang, J.; Wang, C.S.; Xu, X.W. Bacterial community on a Guyot in the Northwest Pacific Ocean influenced by physical dynamics and environmental variables. *J. Geophys. Res. Biogeosci.* **2019**, *124*, 2883–2897. [CrossRef]
31. Jiang, X.-D.; Gong, J.-L.; Ren, J.-B.; Liu, Q.-S.; Zhang, J.; Chou, Y.-M. An interdependent relationship between microbial ecosystems and ferromanganese nodules from the Western Pacific Ocean. *Sediment. Geol.* **2020**, *398*, 105588. [CrossRef]
32. Nitahara, S.; Kato, S.; Usui, A.; Urabe, T.; Suzuki, K.; Yamagishi, A. Archaeal and bacterial communities in deep- sea hydrogenetic ferromanganese crusts on old seamounts of the northwestern Pacific. *PloS ONE* **2017**, *12*, e0173071. [CrossRef]
33. Granina, L.Z. *Early Diagenesis in Bottom Sediments of Lake Baikal*; Academic Publishing House Geo: Novosibirsk, Russia, 2008; 159p.
34. Nealson, K.H. The manganese-oxidizing bacteria. *Prokaryotes* **2006**, *5*, 222–231. [CrossRef]
35. Tebo, B.M.; Bargar, J.R.; Clement, B.G.; Dick, G.J.; Murray, K.J.; Parker, D.L.; Verity, R.; Webb, S.M. Biogenic manganese oxides: Properties and mechanisms of formation. *Annu. Rev. Earth Planetary. Sci.* **2004**, *32*, 287–328. [CrossRef]
36. Tebo, B.M.; Johnson, H.A.; McCarthy, J.K.; Templeton, A.S. Geomicrobiology of manganese(II) oxidation. *Trends Microbiol.* **2005**, *13*, 421–428. [CrossRef] [PubMed]
37. Strakhovenko, V.; Shkol'nikc, S.I.; Danilenkoa, I.V. Ferromanganese nodules of freshwater reservoirs of Ol'khon Island (Baikal) and the Kulunda Plain (West Siberia). *Russ. Geol. Geophys.* **2018**, *59*, 123–134. [CrossRef]
38. Dedysh, S.N.; Kulichevskaya, I.S.; Serkebaeva, Y.M.; Mityaeva, M.A.; Sorokin, V.V.; Suzina, N.E.; Rijpstra, W.I.; Damsté, J.S. *Bryocella elongata* gen. nov., sp. nov., a member of subdivision 1 of the *Acidobacteria* isolated from a methanotrophic enrichment culture, and emended description of *Edaphobacter aggregans* Koch et al. 2008. *Int. J. Syst. Evol. Microbiol.* **2012**, *62*, 654–664. [CrossRef] [PubMed]
39. Gorlenko, V.M.; Dubinina, G.A.; Kuznetsov, S.I. *Ecology of Aquatic Organisms*; Nauka: Moscow, Russia, 1977; 289p.
40. Sommers, M.; Dollhopf, M.; Douglas, S. Freshwater ferromanganese stromatolites from Lake Vermilion, Minnesota: Microbialculturing and environmental scanning electron microscopy investigations. *Geomicrobiol. J.* **2002**, *19*, 407–427. [CrossRef]
41. Hirano, S.; Ito, Y.; Tanaka, S.; Nagaoka, T.; Oyama, T. Microbial community composition in iron deposits and manganese crusts formed in riverine environments around the Aso area in Japan. *Res. Microbiol.* **2020**, *171*, 271–280. [CrossRef]
42. Dittrich, M.; Moreau, L.; Gordon, J.; Quazi, S.; Palermo, C.; Fulthorpe, R.; Katsev, S.; Bollmann, J.; Chesnyuk, A. Geomicrobiology of iron layers in the sediment of Lake Superior. *Aquat. Geochem.* **2015**, *21*, 123–140. [CrossRef]
43. Hauck, S.; Benz, M.; Brune, A.; Schink, B. Ferrous iron oxidation by denitrifying bacteria in profundal sediments of a deep lake (Lake Constance). *FEMS Microbiol. Ecol.* **2001**, *37*, 127–134. [CrossRef]
44. Huo, Y.; Cheng, H.; Anton, F.; Wang, C.; Jiang, X.; Pan, J.; Wu, M.; Xu, X. Ecological functions of uncultured microorganisms in the cobalt-rich ferromanganese crust of a seamount in the central Pacific are elucidated by fosmid sequencing. *Acta Oceanol. Sin.* **2015**, *34*, 92–113. [CrossRef]
45. Nitahara, S.; Kato, S.; Urabe, T.; Usui, A.; Yamagishi, A. Molecular characterization of the microbial community in hydrogenetic ferromanganese crusts of the Takuyo-Daigo Seamount, northwest Pacific. *FEMS Microbiol. Lett.* **2011**, *321*, 121–129. [CrossRef]
46. Granina, L.; Karabanov, E.; Callender, E. Relics of oxidised ferromanganese formations in the bottom sediments of Lake Baikal. *IPPCCE Newsl.* **1993**, *7*, 32–39.
47. Dubinina, G.A. Study of the ecology of iron bacteria in fresh water basins. *Izv. Acad. Sci. USSR. Ser. Biol.* **1976**, *4*, 575–592. (In Russian)
48. Zakharova, Y.R.; Parfenova, V.V.; Granina, L.Z.; Kravchenko, O.S.; Zemskaya, T.I. Distribution of iron and manganeseoxidizing bacteria in the bottom sediments of Lake Baikal. *Inland Water Biol.* **2010**, *3*, 313–321. [CrossRef]
49. Zemskaya, T.I.; Lomakina, A.V.; Mamaeva, E.V.; Zakharenko, A.S.; Likhoshvai, A.V.; Galachyants, Y.P.; Miller, B. Composition of microbial communities in sediments from southern Baikal containing Fe/Mn concretions. *Microbiology* **2018**, *87*, 382–392. (In Russian) [CrossRef]
50. Bukharov, A.A.; Fialkov, V.A. *The Geologic Structure of the Baikal Bottom*; Nauka: Moscow, Russia, 1996.
51. Manceau, A.; Kersten, M.; Marcus, M.A.; Geoffroy, N.; Granina, L. Ba and Ni speciation in a nodule of binary Mn oxide phase composition from Lake Baikal. *Geoch. Cosmochim. Acta* **2007**, *71*, 1967–1981. [CrossRef]
52. Amirzhanov, B.J.; Pampoura, V.D.; Piskunova, L.F.; Karabanov, E.V. Geochemical Types of Ferromanganese Nodules of Lake Baikal. *Dokl. Akad. Nauk* **1992**, *326*, 530–534. (In Russian)
53. Bukharov, A.A.; Murashko, D.N.; Fialkov, V.A. Iron-manganese nodules on the underwater slope of the Ushkany Islands (Lake Baikal). *Geol. Ore Depos.* **1992**, *34*, 80–91.
54. Takhteev, V.V.; Bukharov, A.A.; Proviz, V.I.; Sitnikova, T.Y.; Galkin, A.N. A peculiarity of bottom fauna within unusual geological environment of the northern slope of Bolshoi Ushkany Island (Lake Baikal). In *Studies of the Fauna in Waters Bodies of Eastern Siberia*; Takhtaeev, V.V., Ed.; Irkutsk University: Irkutsk, Russia, 2001; pp. 3–8.
55. Wetzel, R.G.; Likens, G.E. *Limnological Analyses*; Springer: New York, NY, USA, 1991; 391p. [CrossRef]
56. Baram, G.I.; Vereshchagin, A.L.; Golobokova, L.P. Microcolumn highperformance liquid chromatography with UV detection for the determination of anions in environmental materials. *J. Anal. Chem.* **1999**, *54*, 854–857.
57. McLennan, S.M. Rare Earth Elements in Sedimentary Rocks: Influence of Provenance and Sedimentary Process. *Rev. Mineral.* **1989**, *21*, 169–200.

58. Konstantinova, N.; Hein, J.R.; Gartman, A.; Mizell, K.; Barrules, P.; Cherkashov, G.; Mikhailik, P.; Khanchuk, A. Mineral phase-element associations based on sequential leaching of ferromanganese crusts, Amerasia Basin Arctic Ocean. *Minerals* **2018**, *8*, 460. [CrossRef]
59. Koschinsky, A.; Halbach, P. Sequential leaching of marine ferromanganese precipitates: Genetic implications. *Geochim. Cosmochim. Acta* **1995**, *59*, 5113–5132. [CrossRef]
60. Koschinsky, A.; Hein, J.R. Uptake of elements from seawater by ferromanganese crusts: Solid-phase associations and seawater speciation. *Mar. Geol.* **2003**, *198*, 331–351. [CrossRef]
61. Mikhailik, P.E.; Mikhailik, E.V.; Zarubina, N.V.; Blokhin, M.G. Distribution of rare-earth elements and yttrium in hydrothermal sedimentary ferromanganese crusts of the Sea of Japan (from phase analysis results). *Russ. Geol. Geophys.* **2017**, *58*, 1530–1542. [CrossRef]
62. Kuznetsov, V.; Cherkashev, G.; Lein, A.; Shilov, V.; Maksimov, F.; Arslanov, K.; Stepanova, T.; Baranova, N.; Chernov, S.; Tarasenko, D. 230Th/U dating of massive sulfides from the Logatchev and Rainbow hydrothermal fields (Mid-Atlantic Ridge). *Geochronometria* **2006**, *25*, 51–56.
63. Bol'shakov, A.M.; Egorov, A.V. On the application of phase equilibrium degassing for gasometric research in water areas. *Okeanologiya* **1987**, *37*, 861–862. (In Russian)
64. Sambrook, J.; Fritsch, E.F.; Maniatis, T. *Molecular Cloning: A Laboratory Manual*; Cold Spring Harbor Laboratory Press: Long Island, NY, USA, 1987.
65. Sahm, K.; John, P.; Nacke, H.; Wemheuer, B.; Grote, R.; Daniel, R.; Antranikian, G. High abundance of heterotrophic prokaryotes in hydrothermal springs of the Azores as revealed by a network of 16S rRNA gene-based methods. *Extremophiles* **2013**, *17*, 649–662. [CrossRef]
66. Yu, Y.; Lee, C.; Kim, J.; Hwang, S. Group-specific primer and probe sets to detect methanogenic communities using quantitative real-time polymerase chain reaction. *Biotechnol. Bioeng.* **2005**, *89*, 670–679. [CrossRef]
67. Bolger, A.M.; Lohse, M.; Usadel, B. Trimmomatic: A flexible trimmer for Illumina sequence data. *Bioinformatics* **2014**, *30*, 2114–2120. [CrossRef]
68. Andrews, S. FastQC: A Quality Control Tool for High throughput Sequence Data. 2020. Available online: http://www.bioinformatics.babraham.ac.uk/projects/fastqc (accessed on 1 February 2022).
69. Schloss, P.D.; Westcott, S.L.; Ryabin, T.; Hall, J.R.; Hartmann, M.; Hollister, E.B.; Lesniewski, R.A.; Oakley, B.B.; Parks, D.H.; Robinson, C.J.; et al. Introducing mothur: Opensource, platform-independent, community-supported software for describing and comparing microbial communities. *Appl. Environ. Microbiol.* **2009**, *75*, 7537–7541. [CrossRef]
70. Edgar, R.C.; Haas, B.J.; Clemente, J.C.; Quince, C.; Knight, R. UCHIME improves sensitivity and speed of chimera detection. *Bioinformatics* **2011**, *27*, 2194–2200. [CrossRef]
71. Kozich, J.J.; Westcott, S.L.; Baxter, N.T.; Highlander, S.K.; Schloss, P.D. Development of a dual-index sequencing strategy and curation pipeline for analyzing amplicon sequence data on the MiSeq Illumina sequencing platform. *Appl. Environ. Microbiol.* **2013**, *79*, 5112–5120. [CrossRef] [PubMed]
72. R Core Team. R: A Language and Environment for Statistical Computing. 2022. Available online: https://www.R-project.org/ (accessed on 4 April 2022).
73. Mizell, K.; Hein, J.R.; Au, M.; Gartman, A. Estimates of metals contained in abyssal manganese nodules and ferromanganese crusts in the global ocean based on regional variations and genetic types of nodules. In *Perspectives on Deep-Sea Mining*; Sharma, R., Ed.; Springer: Cham, Switzerland, 2022; pp. 53–80. [CrossRef]
74. Petrov, L.L.; Kornakov, Y.N.; Persikova, L.A.; Anchutina, E.A. Reference samples of Lake Baikal bottom sediments—An essential part of regional collection of reference samples. *Int. J. Environ. Anal. Chem.* **1999**, *74*, 275–288. [CrossRef]
75. Zhmodik, S.M.; Verkhovtseva, N.V.; Soloboeva, E.V.; Mironov, A.G.; Nemirovskaya, N.A.; Ilić, R.; Khlystov, O.M.; Titov, A.T. The study of distribution and forms of uranium occurrences in Lake Baikal sediments by the SSNTD method. *Radiat. Meas.* **2005**, *40*, 532–538. [CrossRef]
76. Och, L.M.; Müller, B.; März, C.; Wichser, A.; Vologina, E.G.; Sturm, M. Elevated uranium concentrations in Lake Baikal sediments: Burial and early diagenesis. *Chem. Geol.* **2016**, *441*, 92–105. [CrossRef]
77. Coates, J.D.; Ellis, D.J.; Gaw, C.V.; Lovley, D.R. *Geothrix fermentans* gen. nov., sp. nov., a novel Fe(III)-reducing bacterium from a hydrocarbon-contaminated aquifer. *Int. J. Syst. Bacteriol.* **1999**, *49*, 1615–1622. [CrossRef]
78. Costas, A.M.G.; Liu, Z.; Tomsho, L.P.; Schuster, S.C.; Ward, D.M.; Bryant, D.A. Complete genome of *Candidatus* Chloracidobacterium thermophilum, a chlorophyll-based photoheterotroph from the phylum *Acidobacteria*. *Environ. Microbiol.* **2012**, *14*, 177–190. [CrossRef]
79. Woodcroft, B.J.; Singleton, C.M.; Boyd, J.A.; Evans, P.N.; Emerson, J.B.; Zayed, A.A.F.; Hoelzle, R.D.; Lamberton, T.O.; McCalley, C.K.; Hodgkins, S.B.; et al. Genome-centric view of carbon processing in thawing permafrost. *Nature* **2018**, *560*, 49–54. [CrossRef]
80. Hao, L.; McIlroy, S.J.; Kirkegaard, R.H.; Karst, S.M.; Fernando, W.E.Y.; Aslan, H.; Meyer, R.L.; Albertsen, M.; Nielsen, P.H.; Dueholm, M.S. Novel prosthecate bacteria from the candidate phylum Acetothermia. *ISME J.* **2018**, *12*, 2225–2237. [CrossRef]
81. Tang, Y.J.; Shan, Y.; Zhuang, W.-Q.; Zinder, S.H.; Keasling, J.D.; Alvarez-Cohen, L. Investigation of carbon metabolism in "*Dehalococcoides ethenogenes*" strain 195 by use of isotopomer and transcriptomic analyses. *J. Bacteriol.* **2009**, *191*, 5224–5231. [CrossRef]

82. Cabello-Yeves, P.J.; Zemskaya, T.I.; Zakharenko, A.S.; Sakirko, M.V.; Ivanov, V.G.; Ghai, R.; Rodriguez-Valera, F. Microbiome of the deep Lake Baikal, a unique oxic bathypelagic habitat. *Limnol. Oceanogr.* **2020**, *65*, 1471–1488. [CrossRef]
83. Becraft, E.D.; Woyke, T.; Jarett, J.; Ivanova, N.; Godoy-Vitorino, F.; Poulton, N. Rokubacteria: Genomic giants among the uncultured bacterial phyla. *Front. Microbiol.* **2017**, *8*, 2264. [CrossRef]
84. Zemskaya, T.I.; Bukin, S.V.; Lomakina, A.V.; Pavlova, O.N. Microorganisms in the sediments of Lake Baikal, the deepest and oldest lake in the world. *Microbiology* **2021**, *90*, 286–303. (In Russian) [CrossRef]
85. Lomakina, A.V.; Mamaeva, E.V.; Galachyants, Y.P.; Petrova, D.P.; Pogodaeva, T.V.; Shubenkova, O.V.; Khabuev, A.V.; Morozov, I.V.; Zemskaya, T.I. Diversity of Archaea in bottom sediments of the discharge areas with oil- and gas-bearing fluids in Lake Baikal. *Geomicrobiol. J.* **2018**, *35*, 50–63. [CrossRef]
86. Walker, C.B.; Torre, J.R.; Klotz, M.G.; Urakawa, H.; Pinel, N.; Arp, D. *Nitrosopumilus maritimus* genome reveals unique mechanisms for nitrification and autotrophy in globally distributed marine crenarchaea. *Proc. Natl. Acad. Sci. USA* **2010**, *107*, 8818–8823. [CrossRef] [PubMed]
87. Aylward, F.O.; Alyson, E.S. Heterotrophic *Thaumarchaea* with small genomes are widespread in the dark Ocean. *mSystems* **2020**, *5*, e00415–e00420. [CrossRef] [PubMed]
88. Northup, D.E.; Barns, S.M.; Yu, L.E.; Spilde, M.N.; Schelble, R.T.; Dano, K.E.; Crossey, L.J.; Connolly, C.A.; Boston, P.J.; Natvig, D.O.; et al. Diverse microbial communities inhabiting ferromanganese deposits in Lechuguilla and Spider Caves. *Environ. Microbiol.* **2003**, *5*, 1071–1086. [CrossRef]
89. Kadnikov, V.V.; Mardanov, A.; Beletsky, A.V.; Shubenkova, O.V.; Pogodaeva, T.N.; Zemskaya, T.I.; Ravin, N.V.; Skryabin, K.G. Microbial community structure in methane hydrate-bearing sediments of freshwater Lake Baikal. *FEMS Microbiol. Ecol.* **2012**, *79*, 348–358. [CrossRef]
90. Gebers, R.; Beese, M. *Pedomicrobium americanum* sp. nov. and *Pedomicrobium australicum* sp. nov. from aquatic habitats, *Pedomicrobium* gen. emend., and *Pedomicrobium ferrugineum* sp. emend. *Int. J. Syst. Bacteriol.* **1988**, *38*, 303–315. [CrossRef]
91. Sujith, P.P.; Gonsalves, M.J.B.D.; Bhonsle, S.; Shaikh, S.; LokaBharathi, P.A. Bacterial activity in hydrogenetic ferromanganese crust from the Indian Ocean: A combined geochemical, experimental and pyrosequencing study. *Environ. Earth Sci.* **2017**, *76*, 191. [CrossRef]
92. Sujith, P.P.; Gonsalves, M.J.B.D. Ferromanganese oxide deposits: Geochemical and microbiological perspectives of interactions of cobalt and nickel. *Ore Geol. Rev.* **2021**, *139*, 104458. [CrossRef]
93. Yuling, L.; Boqing, T.; Yuanxinglu, L.; Ming, L.; Xiangdong, W.; Xiaoli, L.; Huihui, D. Inoculation of soil with cadmium-resistant bacterium *Delftia* sp. B9 reduces cadmium accumulation in rice (*Oryza sativa* L.) grains. *Ecotoxicol. Environ. Saf.* **2018**, *163*, 223–229. [CrossRef]
94. Diels, L.; Geets, J.; Dejonghe, W.; Van Roy, S.; Vanbroekhoven, K.; Szewczyk, A.; Malina, G. Heavy metal immobilization in groundwater by in situ bioprecipitation: Comments and questions about efficiency and sustainability of the process. *Proc. Annu. Int. Conf. Soils Sediments Water Energy* **2010**, *11*, 7. Available online: https://scholarworks.umass.edu/soilsproceedings/vol11/iss1/7 (accessed on 1 February 2022).
95. Daims, H.; Nielsen, J.L.; Nielsen, P.H.; Schleifer, K.H.; Wagner, M. In situ characterization of *Nitrospira*-like nitrite-oxidizing bacteria active in wastewater treatment plants. *Appl. Environ. Microbiol.* **2001**, *67*, 5273–5284. [CrossRef] [PubMed]
96. Mori, K.; Sunamura, M.; Yanagawa, K.; Ishibashi, J.; Miyoshi, Y.; Iino, T.; Suzuki, K.; Urabe, T. First cultivation and ecological investigation of a bacterium affiliated with the Candidate Phylum OP5 from Hot Springs. *Appl. Environ. Microbiol.* **2008**, *74*, 6223–6229. [CrossRef] [PubMed]
97. Zhang, Y.X.; Dong, C.; Biao, S. *Planiflum yunnanense* sp nov., a thermophilic thermoactinomycete isolated from a hot spring. *Int. J. Syst. Evol. Microbiol.* **2007**, *57*, 1851–1854. [CrossRef] [PubMed]
98. Vuillemin, A.; Kerrigan, Z.; D'Hondt, S.; Orsi, W.D. Exploring the abundance, metabolic potential and gene expression of subseafloor Chloroflexi in million-year-old oxic and anoxic abyssal clay. *FEMS Microbiol. Ecol.* **2020**, *96*, fiaa223. [CrossRef]
99. Ward, L.M.; Idei, A.; Nakagawa, M.; Ueno, Y.; Fischer, W.W.; McGlynn, S.E. Geochemical and metagenomics characterization of Jinata Onsen, a Proterozoic-analog hot spring, reveals novel microbial diversity including iron-tolerant phototrophs and thermophilic lithotrophs. *Microbes Environ.* **2019**, *34*, 278–292. [CrossRef]
100. Colman, S.M.; Nicholsm, D.R.; Badardinov, A.A.; Foster, D.S.; O'Toole, J.K.; Parolski, K.E. High-resolution seismic-reflection surveys of Lake Baikal, Siberia 1990–1992: Methods and examples. International Project on Paleolimnology and Late Cenozoic Climate. *IPPCCE Newsl.* **1993**, *7*, 43–48.
101. Vologina, E.G.; Sturm, M.; Vorobyova, S.S.; Granina, L.Z. New results of high-resolution studies of surface sediments of Lake Baikal. *Terra Nostra* **2000**, *9*, 115–131.
102. Cronan, D.S. Manganese Nodules. In *Earth Systems and Environmental Sciences*, 3rd ed.; Steele, J.H., Ed.; Academic Press: Cambridge, MA, USA, 2018; Volume 5, pp. 607–614. [CrossRef]
103. Han, X.; Schubert, C.J.; Fiskal, A.; Dubois, N.; Lever, M.A. Eutrophication as a driver of microbial community structure in lake sediments. *Environ. Microbiol.* **2020**, *22*, 3446–3462. [CrossRef]
104. Wurzbacher, C.; Nilsson, R.H.; Rautio, M.; Peura, S. Poorly known microbial taxa dominate the microbiome of permafrost thaw ponds. *ISME J.* **2017**, *11*, 1938–1941. [CrossRef] [PubMed]

105. Shiraishi, F.; Mitsunobu, S.; Suzuki, K.; Hoshino, T.; Morono, Y.; Inagaki, F. Dense microbial community on a ferromanganese nodule from the ultra-oligotrophic South Pacific Gyre: Implications for biogeochemical cycles. *Earth. Planet. Sci. Lett.* **2016**, *447*, 10–20. [CrossRef]
106. Kielak, A.M.; Barreto, C.C.; Kowalchuk, G.A.; van Veen, J.A.; Kuramae, E.E. The ecology of *Acidobacteria*: Moving beyond genes and genomes. *Front. Microbiol.* **2016**, *7*, 744. [CrossRef] [PubMed]
107. Wear, E.K.; Church, M.J.; Orcutt, B.N.; Shulse, C.N.; Lindh, M.V.; Smith, C.R. Bacterial and Archaeal communities in polymetallic nodules, sediments, and bottom waters of the abyssal clarion-clipperton zone: Emerging patterns and future monitoring considerations. *Front. Mar. Sci.* **2021**, *8*, 634803. [CrossRef]
108. Torres, N.T.; Och, L.M.; Hauser, P.C.; Furrer, G.; Brandl, H.; Vologina, E.; Sturm, M.; Burgmann, H.; Beat Muller, B. Early diagenetic processes generate iron and manganese oxide layers in the sediments of Lake Baikal, Siberia. *Environ. Sci.* **2014**, *16*, 879–889. [CrossRef]
109. Castelle, C.J.; Brown, C.T.; Anantharaman, K.; Probst, A.J.; Huang, R.H.; Banfield, J.F. Biosynthetic capacity, metabolic variety and unusual biology in the CPR and DPANN radiations. *Nat. Rev. Microbiol.* **2018**, *16*, 629–645. [CrossRef]
110. Liu, X.; Wang, Y.; Gu, J.-D. Ecological distribution and potential roles of Woesearchaeota in anaerobic biogeochemical cycling unveiled by genomic analysis. *Comput. Struct. Biotechnol. J.* **2021**, *19*, 794–800. [CrossRef]
111. Berg, J.S.; Jerˊzerˊque, D.; Duverger, A.; Lamy, D.; Laberty-Robert, C.; Miot, J. Microbial diversity involved in iron and cryptic sulfur cycling in the ferruginous, low-sulfate waters of Lake Pavin. *PLoS ONE* **2019**, *14*, e0212787. [CrossRef]
112. Crowe, S.A.; Maresca, J.A.; Jones, C.; Sturm, A.; Henny, C.; Fowle, D.A.; Cox, R.P.; Delong, E.F.; Canfield, D.E. Deep-water anoxygenic photosythesis in a ferruginous chemocline. *Geobiology* **2014**, *12*, 322–339. [CrossRef]
113. Hansel, C.M.; Lentini, C.J.; Tang, Y.; Johnston, D.T.; Wankel, S.D.; Jardine, P.M. Dominance of sulfur-fueled iron oxide reduction in low-sulfate freshwater sediments. *ISME J.* **2015**, *9*, 2400–2412. [CrossRef]
114. Granina, L.Z.; Mats, V.D.; Phedorin, M.A. Iron-manganese formations in the Baikal region. *Russ. Geol. Geophys.* **2010**, *51*, 650–660. [CrossRef]
115. Soyol-Erdene, T.-O.; Huh, Y. Rare earth element cycling in the pore waters of the Bering Sea Slope (IODP Exp. 323). *Chem. Geol.* **2013**, *358*, 75–89. [CrossRef]